Published in "Chemistry – A European Journal 21(10): 3854–3874, 2015"
which should be cited to refer to this work.

Nanorattles or Yolk–Shell Nanoparticles—What Are They, How Are They Made, and What Are They Good For?

Magdalena Priebe* and Katharina M. Fromm*[a]

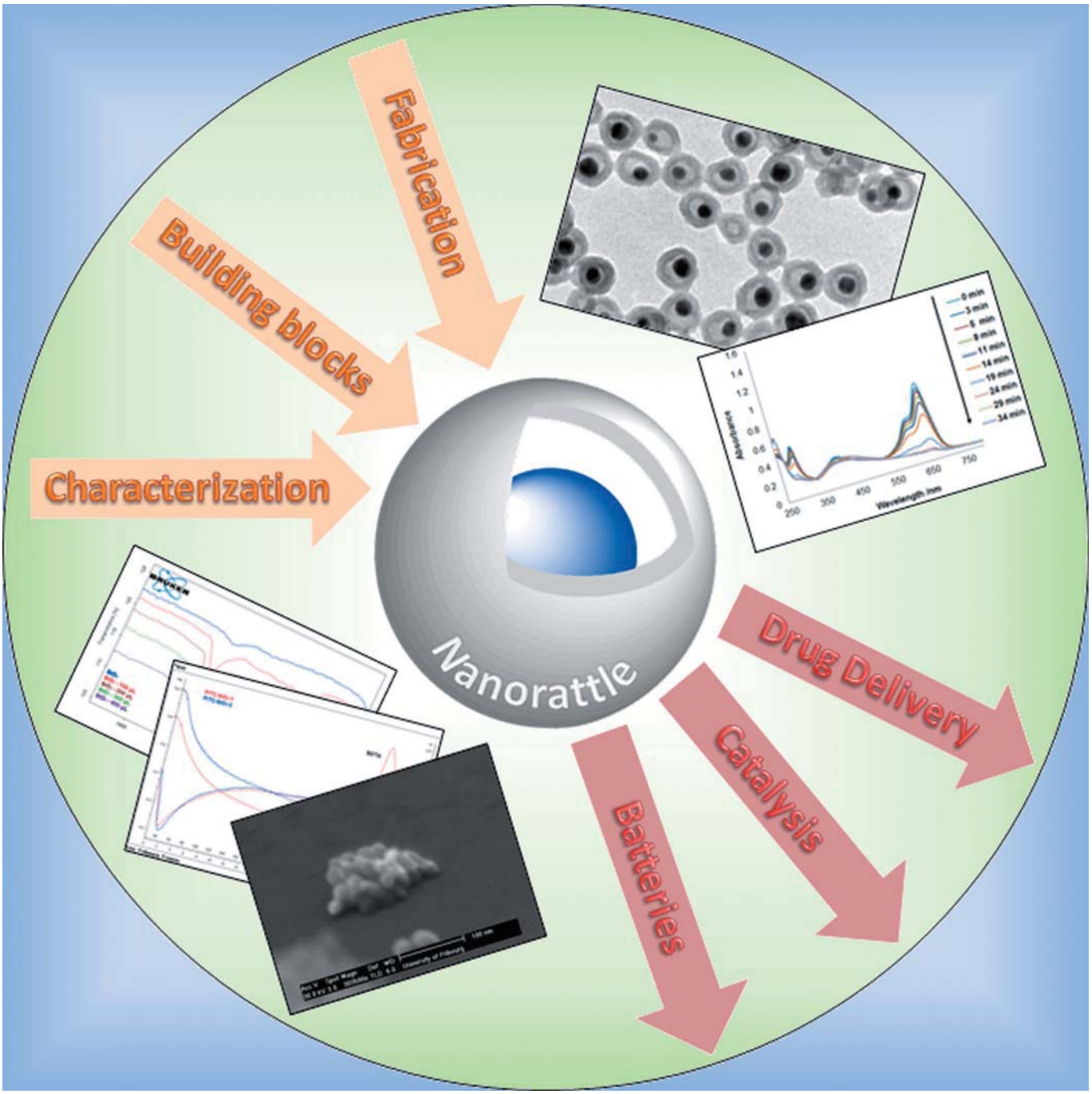

Abstract: The development of nanotechnology has led to the design of cutting-edge nanomaterials with increasing levels of complexity. Although "traditional" solid, uniform nanoparticles are still the most frequently reported structures, new generations of nanoparticles have been constantly emerging over the last several decades. The outcome of this nano-art extends beyond nanomaterials with alternative compositions and/or morphologies. The current state-of-the-art allows for the design of nanostructures composed of different building blocks that exhibit diverse properties. Furthermore, those properties can be a reflection of either individual features, which are characteristic of a particular building block alone, and/or synergistic effects resulting from interactions between building blocks. Therefore, the unique structures as well as the outstanding properties of nanorattles have attracted increasing attention for possible biomedical and industrial applications. Although these nanoparticles resemble core–shell particles, they have a distinctive feature, which is a presence of a void that provides a homogenous environment for the encapsulated core. In this Review, we give a comprehensive insight into the fabrication of nanorattles. A special emphasis is put on the choice of building blocks as well as the choice of preparation method, because those two aspects further influence properties and thus possible future applications, which will also be discussed.

1. Introduction to Nanorattles

The first visionary outlook for the development of nanotechnology dates back to December 1959 when Richard Feynman gave his eminent talk entitled "*There's Plenty of Room at the Bottom*".[1] Although the term nanotechnology was not utilized at that time and it has taken decades for Feynman's visions to become respected and partially realized,[2] humanity has certainly been fabricating and using nanoparticles since ancient times without even realizing it. The prime example is the Lycurgus cup—a fabulous cup dating back to the 4th century A.D. made of dichroic glass that changes color depending on whether light is reflected or transmitted. These extraordinary properties originate from the presence of gold–silver alloy nanoparticles with a diameter of 50–100 nm, and were the masterstroke of ancient Roman glassmakers.[3]

With the development of electron-microscopy techniques, a "micro and nano fever" swept the scientific world.[2] On one hand, there has been an interest in preparing finer and finer particles with variable properties depending on their size and shape.[4] On the other hand, considerable focus has been put on the development of fancy structures.[5] As numerous reviews on nanoparticles have already been published,[6,7] the authors of this work would like to present a review solely on the nanorattle type of nanomaterials, also frequently called yolk–shell nanoparticles. These structures should be distinguished from solid nanoparticles[8–12] (composed of one or many elements, but with a uniform structure), Janus particles[13] (two parts of the particle have different chemical or physical properties), hollow particles[9–11,14] (with an empty interior), core–shell particles[8,12,15] (comprising smaller solid particle(s) coated with a tight layer of other element(s)), as well as from reverse bumpy balls[16,17] (encapsulated cores attached to the shell). As shown in Figure 1, the feature differentiating nanorattles[8–10,12,14,15] from the aforementioned structures is the void between the encapsulated cargo and the surrounding shell. This is clearly a generalization, because more than one particle can be encapsulated in the cavity[9,18–20] or the shell can be composed of several cavities with single particles inside.[21] Additionally, the shell can be constituted of multiple layers[8,22–25] and contain functional groups[26,27] or targeting moieties.[27] With regard to shape, spheres[9,14,15,18,23,28–33] are the most frequent; however, other possibilities have been reported as well. These include spindle,[34,35] rodlike,[20,36,37] and cubic[38–41] nanorattles. Very often the shell adopts the same shape as the core,[33,34] but it is not a general rule.[20,33,39] Last but not least, a core does not necessarily need to be a solid nanoparticle and can be made of hollow sphere(s), resulting in a rattle-type ball-in-ball sphere.[42,43]

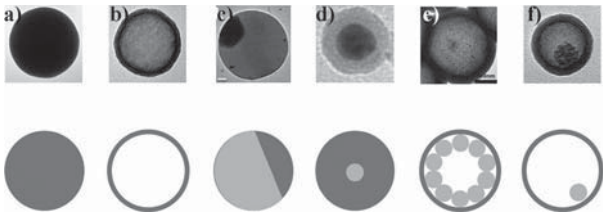

Figure 1. TEM images and schematic representations of the common types of nanoparticles: a) solid, b) hollow, c) Janus,[13a] d) core–shell, e) reverse bumpy ball[17] and f) yolk–shell particle or nanorattle.

Normally, nanorattles are denoted as core@shell, for example Au@$MgSiO_3$,[44] as well as Au@HSNs (for hollow silica nanospheres)[9] but sometimes they are also described as core@void@shell[19,23,45] such as Si@void@C,[19] Pt@void@TiO_2,[46] or Au,@ZrO_2[15] to emphasize the presence of the void. In cases where the shell consists of two layers, the designation takes the form of core@shell1@shell2, such as α-Fe_2O_3@SiO_2@SiO_2,[47] or SnO_2@SnO_2@SnO_2.[24] Herein, the presence of the void will not be additionally indicated and only the denotation core@shell will be used, since mainly rattle structures are considered in the scope of this review.

The principal purpose of encapsulation is to provide protection for the core so that its functionalities are not diminished

[a] *Dr. M. Priebe, Prof. Dr. K. M. Fromm*
Chemistry Department
University of Fribourg
Chemin du Musée 9, 1700 Fribourg (Switzerland)
E-mail: magdalena.priebe@gmail.com
katharina.fromm@unifr.ch

and do not vanish upon aggregation and sintering,[15,21,31,44,48] under harsh reaction conditions,[9,15,21] or through interaction with the surrounding environment.[9,19,30] In many cases, however, the shell provides some important functionalities itself. This can include the presence of reactive sites, such as $-NH_2$ groups, for the attachment of targeting molecules for drug delivery[27,31] or sites for the absorption of target molecules, such as groups aimed at the extraction of organic targets.[30]

Multiple possible applications enabled by nanorattles have become a source of inspiration for scientists to develop the best and most efficient methods for their preparation. Nanorattles can be prepared in numerous ways and a border line is not always lucid. As nanotechnology is a multidisciplinary science gathering researchers from various fields, we will make an attempt to provide general guidelines for the preparation of nanorattles based on the current literature. In the scope of this Review, we categorize those methods depending on 1) the use of a template, 2) the sequence of core and shell formation, 3) the way to obtain a void between core and shell, 4) the importance of building blocks in the design of future applications as well as 5) their characterization methods. In the following subchapters, we will show that a vast number of possible nanorattles can be fabricated with combinations of the diverse functionalities of their components (see section 2. Nanorattle Building Blocks). This can clearly be achieved by several different approaches (see section 3. Methods for the Fabrication of Nanorattles) influencing further the properties of the obtained products, such as the dimensions of the compartments. Then, we will emphasize the importance of the nanorattle building blocks in the design of the future applications (section 4) and will show that despite of a variety of analytical methods, the characterization of nanorattles is not always straightforward and complex analysis is often required (section 5). Finally, we will provide some recent examples of nanorattles with potential for practical applications (section 6).

2. Nanorattle Building Blocks

A vast number of possible building blocks provide a variety of compositions for the construction of nanorattles. The core is usually made of metals (Au,[29,31,44,49] Ag,[50–52] Cu,[51] Pt,[28,46] Pd,[21,53] Ni[12]), metalloids (Si[19]), oxides (SiO_2,[10] Fe_2O_3,[31,34] Fe_3O_4,[14,27,54–56] SnO_2,[24] Co_3O_4,[40]), doped oxides (Gd_2O_3:Eu^{3+}[57]) or sulfides (Ag_2S, CdS, PbS, ZnS, $AgInS_2$),[41] whereas the shell can be composed of metal (Pt[49]), oxides (SiO_2,[10,29,31,51] $MgSiO_3$,[44] $CuSiO_3$,[44] $NiSiO_3$,[44] $NiTiO_3$,[45] CeO_2,[21,28] ZrO_2,[15] TiO_2,[46,56] SnO_2,[8,24] Fe_2O_3[52]), polymers[50,58] (P(NIPAm-coAAM),[57] PMAA,[59] PANi[55]) or carbon[58] (C^{18} groups,[30] nitrogen-doped carbon[19]).

The chemical composition of nanorattles largely determines their properties. For example, Au,[9,15,18,31,44,48,60] Ni,[12] and Pd[21,53,61] mainly constitute the core of catalytic nanorattles. Very often, functionality depends solely on the nature of the core[9,12,18] and the function of the shell is reduced to a protecting role.[9,15,18] However, some studies report a synergistic role of both core and shell, as seen for example in Pt@CeO_2,[28] Co_3O_4@SiO_2,[40] or Fe_3O_4@SnO_2[8] resulting in improved visible-light photocatalysis,[28] catalysis,[40] as well as microwave absorption,[8] respectively. Nanorattles with individual functionalities for different compartments are gaining increased attention; for instance, in the combination of a magnetic Fe_3O_4 core and a photocatalytic TiO_2 shell.[56] The presence of pores on the surface of shells provides channels through which small molecules can enter the cavity.[40] This aspect should be especially kept in mind when nanorattles are intended to act as drug carriers or nanoreactors, as pore blockage can diminish the overall performance. Although still neglected, the void also seems to play a crucial role in determining the final properties.[34]

As nanorattles are complex structures and still remain a relatively new type of nanomaterial, a lot of effort is focused on the utilization of well-understood processes for their preparation. Sol-gel processes to obtain silica have been intensively investigated over the last decades and are commonly used in the preparation of nanostructures.[62] Owing to the well-known silica chemistry, as well as a variety of benefits served by its numerous precursors, it is still the most broadly used composite for the preparation of nanorattles. Table 1 shows the most important silica precursors used in the preparation of nanorattles. Only two of those (TEOS and TMOS) contain four hydrolyzable groups, whereas all others have only three hydrolyzable groups and one remaining substituent. This substituent provides some unique properties, allowing the design of nanorattles. First, the precursors shown in Table 1 differ in the rate of hydrolysis and condensation,[14,29] a fact that results in a change in the density of the siloxane framework. It was re-

Katharina M. Fromm obtained her PhD from the University of Karlsruhe, Germany, in 1994. After postdoctoral studies in solid-state chemistry (J. Strähle, Tübingen) and supramolecular chemistry (J.-M. Lehn, Strasbourg), she obtained her habilitation from the University of Geneva, Switzerland, in 2002. An Emmy-Noether II project by the DFG and a Swiss National Science Foundation Research Professorship allowed her to build up her own group. She has held the position of full professor at the University of Fribourg since 2006, and was elected in 2011 as research councilor of the Swiss National Science Foundation. In 2013, she was awarded as fellow of the American Chemical Society.

Magdalena Priebe was born in Poznan, Poland, in 1985. She obtained her Master's degree in Commodity Sciences from Poznan University of Economics in 2009. In 2014, she received her PhD in chemistry from the University of Fribourg, Switzerland, under the supervision of Prof. Katharina M. Fromm for her work on the microemulsion approach to the design of multifunctional nanocontainers and nanorattles.

Table 1. Silica precursors used in the preparation of nanorattles.

Acronym	Full name	References
TEOS	tetraethyl orthosilicate, tetraethoxysilane, tetraethylorthosilane	[9, 14, 18, 20, 23, 26, 27, 29–31, 34, 40, 44, 54, 57, 66–68]
TMOS	tetramethyl orthosilicate	[12, 53, 69]
APTES	(3-aminopropyl) triethoxysilane	[26, 29]
APTMS	(3-aminopropyl) trimethoxysilane	[9, 14]
BTME	1,2-bis(trimethoxysilyl) ethane	[23, 69]
BTEB	1,4-bis(triethoxysilyl)benzene	[69]
C_{18}TMS	*n*-octadecyl trimethoxysilane	[12, 27, 31]
C_{18}TES	*n*-octadecyl triethoxysilane	[30]
IBMS	isobutyltrimethoxy silane	[70]
MPTMS	(3-mercaptopropyl) trimethoxysilane	[23, 29]
PDES	1*H*, 1*H*, 2*H*, 2*H*-perfluoro decyltriethoxysilane	[29]
PEG-silane	polyethyleneglycol silane	[27]
PMTMS	3-(trimethoxysilyl) propyl methacrylate	[29, 31]
MPS	[3-(methacryloyloxy) propyl]trimethoxy silane	
3-TBS	3-*tert*-butyloxycarbonyl aminopropyl-triethoxysilane	[23]
TMAPS	*N*-trimethoxysilylpropyl-*N,N,N*-trimethylammonium chloride	[22]
TPI	(3-isocyanatopropyl) triethoxysilane	[31]
TSD	*N*-[3-(trimethoxysilyl)propyl]ethylene diamine	[10, 18, 29, 68]

ported, for example, that hydrolysis of TEOS leads to the formation of a more dense silica network than hydrolysis and polycondensation of TEOS together with APTES.[63] This possibility to tune the density is frequently used to selectively remove the silica core[29] or the interlayer between core and shell.[10, 15, 26, 27, 60] Organosiloxanes with longer carbon chains exhibit the ability to influence the pore size of the silica shell.[10, 12, 29, 31] Depending on the substituent (group R), surface properties such as the zeta potential[10] or the hydrophobicity[27, 29, 30] of certain compartments, such as the outer layer[29] and the void,[27, 30] can be altered. In addition, amino silanes, such as APTES, can be used as both vesicle-inducing as well as co-structure directing agents,[22] whereas silanes with long carbon chains, such as C_{18}TMS, act as pore directing agents.[27, 31] And last but not least, R serves as a moiety for surface functionalization. Owing to the presence of $-NH_2$ groups, APTES[14, 26] and APTMS[10, 57] are often used for functionalization of the shell with fluorescent dyes by coupling, for example, with the thioisocyanate group of fluorescein isothiocyanate.[10, 14] The so-prepared fluorescent silica precursors can be either used to coat already synthetized nanorattles through silane coupling[26, 57] or directly in the synthesis of nanorattles during hydrolysis and polycondensation with other silica precursors.[14] As nitrogen-containing molecules can coordinate to metal ions, such as gold ions,[64] they can also be used in the encapsulation of gold by forming a gold complex followed by reduction to metallic gold.[9, 18, 29] For example, when *N*-[3-(trimethoxysilyl)propyl]ethylenediamine (TSD) was used as the amine source, the reduction was carried out solely by heating and no additional reducing agent was necessary.[18, 29] However, in case of shorter carbon chains, such as in APTMS, an additional reducing agent, for example, $NaBH_4$ was required to obtain the Au nanoparticles (NPs).[9] This might be related to structural differences between TSD and APTMS with regard to the number of nitrogen atoms. As the former contains two N atoms, it can form chelates with gold, whereas the latter contains only one site for interaction and the complexation is weaker. Polymers such as polyethylene glycol (PEG) can also be attached to the silica surface either by incorporation of PEG by silanization directly with PEG-silane[27] or by reaction between the amine group on the shell surface with methoxy poly(ethylene glycol) succinimidyl carbonate (mPEG-SC).[26] Another possibility to change the properties of the surface is the oxidation of −SH groups originating from (3-mercaptopropyl)trimethoxysilane into $-SO_3H$ or the deprotection of 3-*tert*-butyloxycarbonyl aminopropyl–triethoxysilane, leading to the presence of $-NH_2$ groups.[23] An extensive review by Sapsford et al. provides useful guidelines for the functionalization of nanoparticles with biological molecules,[65] techniques that certainly can be applied to nanorattles as well.

3. Methods for the Fabrication of Nanorattles

The preparation of nanorattles is hardly ever performed in a single-step synthesis.[24, 32] Usually, the procedure involves several steps including the fabrication of the core, growth of the shell, as well as various post-synthesis treatments such as core removal, functionalization of compartments, and loading with cargo (drug or metal precursors for top-down synthesis of metal@shell nanorattles). Owing to multistep and complex approaches that are often intertwined, the strict classification of fabrication methods is difficult. Herein, we present some guidelines that might be helpful in the decision-making process with regard to the choice of the method for the preparation of a functional nanorattle. While planning the fabrication of nanorattles, three major questions should be answered:

1 Which template should be used?
2 Which compartment of the nanorattle should be fabricated first? Core or shell?
3 How to obtain the desired void between core and shell in cases where core–shell particles are an intermediate form?

3.1. Use of a template

In general, the synthesis can be classified depending on whether a template is used or not. In the former case, either a hard or a soft template constitutes a scaffold for the growth

of the shell. In the latter case, the shell occurs as a result of physical transformations of intermediate templates.

3.1.1. Hard template methods

The hard template method is the most frequently used method[29,30,44,55,56] for the synthesis of hollow spheres and nanorattles owing to its relative simplicity compared with other methods. In a typical procedure (Figure 2), a core

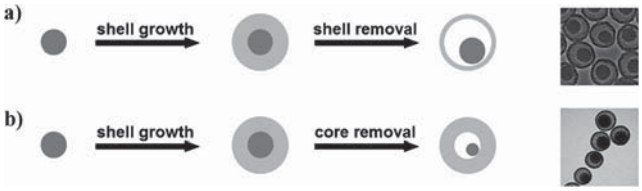

Figure 2. Hard template approach to the preparation of nanorattles. The void is obtained by a) removal of the interlayer[31] and b) partial removal of the core.[30]

(metal,[15,31,44] oxide,[27,29–31,55,56] polymer[71,72]) is coated with one[15,29,55,56] or a few[27,30,31] layers, forming the shell. This coating can be based on the hydrolysis and condensation of silica,[15,27,29,31,44,56] seeded distillation–precipitation polymerization,[31] or a hydrothermal reaction.[30] Subsequently, the core[29,30] or the middle layer[15,27,31,55,56] is removed, leading to a rattle-type structure (see section 3.3 Void Formation).

Using the hard template method, Wu et al. showed the multistep preparation of Fe_3O_4 inside mesoporous silica spheres. Initially, hematite nanoparticles (Fe_2O_3) were coated with silica precursors (TEOS and C_{18}TMS) and then the void between core and shell was obtained upon ammonia etching. Subsequent thermal treatment (at 653 K) in the presence of H_2 (5 vol%)/Ar resulted in the reduction of hematite to magnetite.[27] Linley et al. used silica as an interlayer between a Fe_3O_4 core and a TiO_2 outer shell. Hydrothermal treatment (180 °C, 1.5 h) resulted in the removal of the silica layer as well as a phase change of amorphous TiO_2 into anatase.[56]

An unquestionable advantage of the hard template method is the tunability of the compartments' sizes[8,10,26,31] as well as facile scaling up of the synthesis. If the core is made of silica, its size can be easily controlled in a sol–gel process by simple changes to the reaction parameters. Likewise, the size of the void and the wall thickness can be tuned by the number and the thickness of the layers surrounding the core.[31]

3.1.2. Soft template methods

Soft template methods include the use of microemulsions, surfactants, co-templates, as well as polymers. Although those methods are less frequently used in the fabrication of nanorattles in comparison to the hard template methods, their potential with regard to the preparation of fine homogenous nanocomposites makes them particularly attractive.

3.1.2.1. Microemulsions: The microemulsion technique is a widely used method for the preparation of high-quality nanomaterials,[7,73,74] in which the formation of micelles dictates the size[7,74] and shape[20] of the nanomaterials. As the diameter of the micelles can be tuned simply by changing the water-to-surfactant ratio, controlling the size of nanoparticles is facile.[74] Usually, microemulsions consist of an aqueous phase, an oil phase, and a surfactant, forming ternary systems.[9,74] In the case of quaternary microemulsions,[14,73,75–81] a co-surfactant is additionally added to support the formation of micelles by diminishing the repulsion between the surfactant molecules.[74] Depending on which phase is in the majority, normal (oil-in-water) or reverse (water-in-oil) microemulsions are formed.[7] Solid nanoparticles are fabricated when their precursors are located in the same phase; this can occur either through the mixing and coalescence of two micelles containing different starting materials or by the initiation of a reaction between two precursors in one micelle upon a stimulus, for instance, heating.[73,74] On the other hand, if the reaction is carried out at the boundary of the micelle, hollow spheres can be obtained.[73,74,76,77,79–82] In this case, however, the size of the shell might exceed that of the micelle.[73,74] In addition, to avoid the formation of solid spheres, precursor diffusion into the micelle needs to be decelerated. This can be done by controlling several parameters, such as the choice of the shell precursor, its concentration, temperature and speed of the precursor addition, the temperature of reaction, or the solubility, as well as by increasing the viscosity inside the micelle.[75–80] This method is relatively new for the synthesis of hollow spheres.[73,75,76] Although both normal as well as reversemicelles can be used, the latter ones are more frequently used.[9,14,33,73,74,76–81]

The preparation of nanorattles by using microemulsions can be achieved in three distinct ways. As depicted in Figure 3, this system allows a) the introduction of already prepared NPs[14] or other cargo[74] into the microemulsion and then the growth of a shell around them/it; b) encapsulation of a metal precursor during formation of the shell and reduction to its metallic form after the synthesis of the shell;[9] c) reduction of a metal precursor within the microemulsion and encapsulation of the obtained NPs during the formation of the shell.[33]

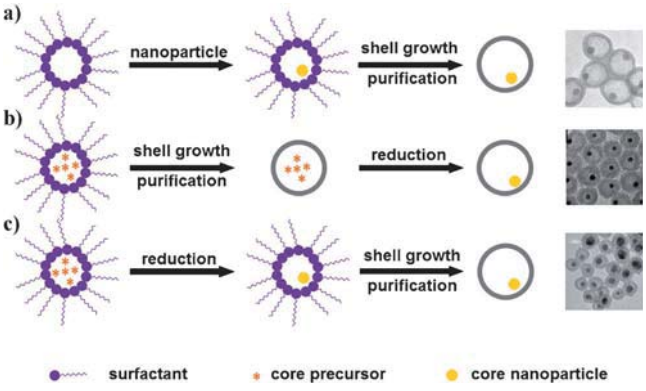

Figure 3. Microemulsion approach to the preparation of nanorattles. Nanorattles are obtained by a) shell growth around a nanoparticle located inside the micelle,[14] b) reduction of metal precursors after growth of the shell,[9] or c) reduction of metal precursors in the micelle and subsequent shell growth.[33]

Feldmann and co-workers have carried out extensive research on the preparation of hollow spheres by using water-in-oil microemulsions stabilized by a cationic surfactant, cetyltrimethylammonium bromide (CTAB)[73,76–81] as well as oil-in-water microemulsions stabilized by an anionic surfactant, sodium dodecyl sulfate (SDS).[73,75] A vast variety of nanocontainers composed of metals (Ag,[80] Au[73,75]), oxides (γ-AlO(OH),[73] $La(OH)_3$,[79] ZnO,[82] SnO_2,[73,81] TiO_2[77]) and sulfides (CuS,[73,78] Cu_2S,[78] $Cu_{1.8}S$[78]) with outer shell diameters of 10–60 nm[74] were prepared. With this method, the dissolution of inorganic salts ($K_2S_2O_8$,[74] KF,[74] KSCN[73]), biomolecules (nicotinic acid,[74] phenylalanine,[73] quercetin[74]) or fluorescent dyes (riboflavin, rhodamine[76]) in the water pool of a reverse micelle prior to shell growth enabled their encapsulation inside AlO(OH).[73,74,76] Although those nanocontainers do not exhibit a yolk–shell structure, they might constitute a basis for the formation of nanostructures of higher complexity, such as nanorattles.

Nanorattles made solely of silica have also been prepared by using the microemulsion approach. Reverse micelles composed of an aqueous phase, cyclohexane and a non-ionic surfactant[9,14,61,83] are the most commonly used system. To obtain hollow SiO_2 spheres, the silica condensation inside the sphere should be reduced. As shown by Lin et al., this can be achieved by proper combination of TEOS and APTMS, where the latter has one less condensable group, the amine group. When TEOS is hydrolyzed and co-condensed together with APTMS at the proper ratio, hollow spheres are obtained. However, if the TEOS/APTMS ratio is too high, or if APTMS is not used at all, solid spheres are obtained instead. Conversely, a too low TEOS/APTMS ratio leads to the destruction of the hollow spheres. It was also shown that changing the sequence of addition of the different ingredients leads to a mixture of small hollow spheres and large yolk–shell spheres.[14] To overcome the problem of size polydispersity, Lin et al. switched from a quaternary microemulsion using Triton X-100 and *n*-hexanol[14] to a ternary system using solely Igepal CO-520[9] as the surfactant.[14] The so-prepared SiO_2 hollow spheres were smaller (diameter = 26.2 ± 2.6 nm, wall thickness = 6 nm) and more monodisperse[9] compared with the previous method (diameter = 40 ± 3.2 nm, wall thickness = 5 nm) when the content of APTS was changed and the surface functionalized with a fluorescent dye. The top-down encapsulation of AuNPs using this method is described in more detail in section 3.2.2.

As mentioned, the microemulsion technique allows the encapsulation of compounds dissolved in the interior of the micelle.[74] In contrast, water-in-oil microemulsions allow the encapsulation of oil-soluble Fe_3O_4 magnetic nanoparticles inside fluorescent silica spheres, even though the silica is formed inside the reverse micelle (i.e., in the water droplet). This is explained by the replacement of the oleylamine protecting group on the Fe_3O_4 surface by hydrolyzed TEOS,[14] which remains in the oil phase before diffusion into the water droplet.[84] Subsequently, the superparamagnetic particles are brought into the micelle. The void between the core and the shell was obtained by soaking the NPs in water for a week.[14] Another example of encapsulation of oil-soluble NiNPs inside SiO_2 by using reverse micelles was shown by Park et al.[12] In this case, however, the void was obtained by selective etching of the metallic core with HCl.[12] The method by which metal particles are dispersed in cyclohexane and are coated in a microemulsion, leading to core–shell particles, followed by subsequent etching of the core or shell is quite common for the formation of nanorattles (Table 2). Moreover, this method often constitutes an intermediate step in the formation of the materials for a further hard template approach. For example, in order to obtain Pd@Niphy (Niphy = nickel phyllosilicate) nanorattles, already prepared PdNPs were coated with silica by using reverse micelles. This yielded Pd@SiO_2 core–shell nanoparticles. Coating with Niphy and subsequent removal of SiO_2 with HF resulted in Pd@Niphy nanorattles.[53]

Table 2. Preparation of nanorattles in microemulsions.

Core	Surfactant	SiO_2 precursor	Removal of	Etching agent	Ref.
Pd	Igepal CO-630	TMOS, C_{18}TMS	Silica layer	H_2O	[61]
Au	Igepal CO-520	TEOS	Fe_3O_4	$NaBH_4$	[83]
Fe_3O_4	Triton X-100	TEOS, APTMS	APTMS	H_2O	[14]
Au	Igepal CO-520	TEOS, APTMS	APTMS	H_2O	[9]
Ag	Igepal CO-520	TEOS, APTMS	APTMS	H_2O	[33]

An interesting approach for the encapsulation of Au@SiO_2 and Ag@SiO_2 was proposed by Yeo et al.[83] As mentioned above, Fe_3O_4 nanoparticles dispersed in cyclohexane can be coated with TEOS. At the same time, Au^{3+} ions from aqueous $HAuCl_4$ solution in the interior of the micelle are reduced by the surfactant and nucleate at the surface of the core. Upon addition of $NaBH_4$, the AuNPs facilitate the reductive dissolution of Fe_3O_4,[83] in which Fe^{III} is probably reduced to more water-soluble Fe^{II},[85] according to the following reaction:[86]

$$Fe_2O_3 + 6\,H^+ + 2\,e^- \rightarrow 2\,Fe^{2+} + 3\,H_2O \quad (1)$$

Removing Fe_3O_4 leads to the formation of Au@SiO_2. Using Fe_3O_4 nanocrystals of different sizes enabled the tuning of the Au@SiO_2 cavity size. Ag@SiO_2 core–shell nanoparticles were obtained by adding $AgNO_3$ and hydrazine to an Au@SiO_2 suspension. By increasing the Ag^+ concentration, it was shown that not only the size of the AgNPs increased but also that nucleation occurred on the Au surface, leading to the encapsulation of AgNPs inside the SiO_2 shell.[83]

Recently, Fan et al. encapsulated hydrophobic $NaYF_4$:Yb/Er@$NaGdF_4$ nanorattles inside a silica shell by using a water-in-oil microemulsion.[67] First, oleic acid-capped cores were suspended in a mixture composed of Igepal CO-520 and cyclohexane (Figure 4). Then, aqueous ammonia was added after 3 h. After another 2 h, TEOS was slowly injected (over 1 hour) into the microemulsion. After 36 h of reaction, samples were purified and a second shell of silica was grown by using the water-phase regrowth method. This was achieved by diluting an aqueous suspension of the silica-coated cores with ethanol and ammonia, followed by slow addition of TEOS over 5 h. The reaction was terminated after 24 h and the samples were puri-

Figure 4. Preparation of nanorattles by encapsulation of the core using a three-step synthesis.

fied. Finally, the rattle structure was obtained by "surface-protected hot water etching". The presence of a protecting agent as well as the etching time were shown to play crucial roles in the formation of the hollow structures. Only the use of poly(vinylpyrrolidinone) (PVP) with a high molecular weight (M_W = 40 000) led to inside-to-outside etching and thus a rattle structure. Using PVP with lower molecular weight (M_W = 10 000) resulted in outside-to-inside etching and no rattles were obtained.[67]

Dahlberg and Schwank reported the synthesis of Ni@SiO_2 nanotubes by using polyoxyethylene (10) cetyl ether as a nonionic surfactant.[20] Conversely to the above-mentioned syntheses, this reaction was carried out at elevated temperatures. The influences of aging time before TEOS addition, of reducing agent concentration, of TEOS concentration, as well as temperature were taken into consideration. It was shown that the silica shell adapts the shape of the micelle. Interestingly, depending on the reaction parameters, shapes varied from spherical to tubular with micrometer length, an observation that was attributed to gas formation contributing to the elongation of the micelles. In the case of micelles where Ni and gas precursors were absent, only a spherical shape was obtained.[20]

In our group, we have modified the microemulsion method proposed by the research group of Mou[9,14] and have developed a one-pot bottom-up synthesis for the preparation of Ag@SiO_2 nanorattles.[33] Contrary to previous studies on reverse micelles,[9,12,14] the cores were prepared directly in the reaction mixture of the microemulsion. First, silver cations were reduced to metallic silver. Depending on the $AgNO_3$ concentration, the size and shape of AgNPs as well as the loading of the nanocontainers could be altered. At lower concentrations (0.001, 0.005, 0.01 M), only few-nanometer spherical AgNPs were obtained. Because of numerous hollow spheres, the yield of the loading was small. However, on increasing the $AgNO_3$ concentration (to 0.05 or 0.1 M), the size of the NPs and the loading of the nanocontainers was increased as well. In addition, shapes other than spherical occurred. In the case of irregular shapes such as rod-like and triangular particles, the shell adapted the shape of the AgNPs. Above 0.15 M $AgNO_3$, the obtained AgNPs were again more homogenous with spherical shape and 100% loading of the nanocontainers with spherical AgNPs was obtained at 0.2 M $AgNO_3$. Further increase of the $AgNO_3$ concentration to 0.5 and 1 M led to core–shell Ag@SiO_2 structures as well as AgNPs embedded in a silica network, respectively.[33] Additionally, the introduction of a fluorescent silica precursor (fluorescein isothiocyanate (FITC)-APTS) allowed the preparation of Ag@FITC-SiO_2 nanorattles.

Recently, Lan et al. reported the synthesis of superparamagnetic nanorattles in a microemulsion composed of two surfactants. In this dual-template strategy, Fe_3O_4/polymethyl methacrylate nanoparticles with an anionic surfactant (sodium dodecylbenzene sulfonate, SDBS) on their surface were dispersed in cationic CTAB. Ultrasonication resulted in the formation of a microemulsion. After growth of the silica shell, the surfactants were removed by alcohol dialysis.[87]

3.1.2.2. Soft co-templates: Song et al. demonstrated the use of a soft co-template as a means to obtain SiO_2@SiO_2 nanorattles with varying sizes and morphologies.[26] Initially, the SiO_2 cores were prepared by modification of the Stöber method.[88] This was achieved by a slow dropwise addition of an ethanolic TEOS solution into a mixture of ammonia, water, and ethanol at 60 °C. After 4 h of reaction, and the subsequent purification and drying, the obtained NPs were dispersed in water and surrounded by vesicles while dispersed in a mixture of CTAB and dodecanol. Further addition of TEOS resulted in the formation of a core–shell–shell structure with two layers of silica that differed in porosity. As the middle layer was more porous, owing to the presence of surfactants, its etching by Na_2CO_3 solution was facilitated. The nanorattles were 200 nm in diameter, and the core size, void size, and wall thickness could be simply controlled by the etching time.[26]

3.1.2.3. Surfactants: The use of surfactants as soft templates was reported for the first time by Wu and Xu. This one-step, general, and simple synthesis employs APTES as a vesicle-inducing agent, and profits from the synergistic effect between zwitterionic (lauryl sulfonate betaine, LSB) and anionic (sodium dodecyl benzenesulfonate) surfactants. After dispersion of the cores in an aqueous mixture of the surfactants, addition of a vesicle-inducing agent, for example, a short-chain alkyl amine, generated the formation of vesicles. Owing to electrostatic attraction, co-structure-directing agents (CSDA) were attached to the vesicle surface. A subsequent sol–gel process with CSDA and TEOS led to the formation of a silica shell replicating the core shape. As this method enables the encapsulation of cores regardless of their size, shape, and chemical composition, spherical SiO_2@SiO_2 and Au@SiO_2 as well as spindle-like Fe_2O_3@SiO_2 nanorattles could be fabricated.[22,35] The preparation of a mesoporous silica shell can be achieved by using a soft template composed of LSB together with SDS, and by replacing APTES by a mixture of APTES and TMAPS as CSDA. In addition, employing yolk–shell particles as the core allows the preparation of SiO_2@SiO_2@SiO_2 nanorattles. In this way, multishelled nanorattles with three or four shells can also be easily prepared (Figure 5).[22]

3.1.2.4. Polymers: Polymers serve an interesting means of soft template that can be used to prepare nanorattles with an organic shell. For example, poly(vinylpyrrolidone) can be effectively used for the preparation of hollow poly(3,4-ethylenedioxythiophene) (PEDOT) through electrochemical polymerization. Subsequent incorporation and reduction of silver cations results in the formation of Ag@PEDOT.[89]

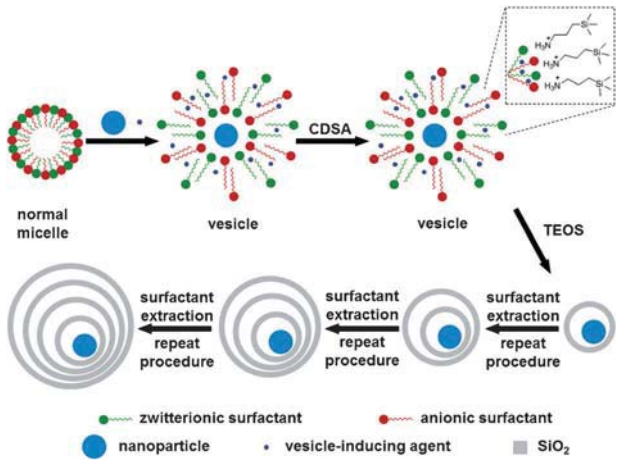

Figure 5. Preparation of multi-shelled nanorattles by using surfactants as soft templates. On the basis of refs. [22] and [35].

3.1.3. Template-free Methods

3.1.3.1. Ostwald ripening: Ostwald ripening is a well-known physical phenomenon in which minuscule crystallites dissolve and recrystallize to form larger ones.[90] Recently, Cao et al. proposed such a mechanism for the formation of "fluffy" core–shell, yolk–shell, and hollow anatase nanoparticles. When amorphous titania spheres were coated with metastable ammonium titanate and subsequently calcinated at 500 °C in air, only the outer layer underwent a phase transition to anatase nanocrystals. Those crystals functioned as seeds for further growth of titania dissolved from the core. As a result of Ostwald ripening, the core was dissolving whereas the shell was enlarging.[91]

Cubic Co_3O_4@SiO_2 nanorattles were prepared by thermal decomposition of $Co_3[Co(CN)_6]_2$@SiO_2 core–shell nanocubes during calcination at 550 °C for 1 h.[40] This thermal treatment led to the conversion of the $Co_3[Co(CN)_6]_2$ nanoparticles to monodisperse Co_3O_4 nanocrystals owing to Ostwald ripening. In addition, due to the high temperatures during this process, the surfaces of the cores were cleaned as well.[40]

Zhang et al. have prepared Pt@CeO_2 yolk–shell spheres by using a template-free hydrothermal method.[28] As PtNPs are necessary to form the spherical CeO_2 shells and because the presence of the void depended on the reaction time as well as on the concentration of the ceria precursor, heterogeneous seeded growth and Ostwald ripening processes both seem to be involved in the mechanism of formation of these particles.[28]

3.1.3.2. Spray pyrolysis: Another template-free approach was proposed by Zheng and co-workers.[32] Various metal@carbon were prepared by ultrasonic spray pyrolysis. In this one-step method, the metal salt is initially reduced by sodium citrate in an aqueous droplet at high temperature. Then, excess sodium citrate forms a shell at the periphery of this hot droplet. Once the shell is carbonized, the carbon shell is obtained. Removal of water-soluble byproducts leads to the formation of nanocontainers with multiple encapsulated cores. As different aqueous solutions can be used, this method allows the encapsulation of different metal nanoparticles to form metal@carbon nanorattles, such as Sn@carbon, Pt@carbon, Ag@carbon, and Fe–FeO@carbon. Interestingly, the loading can be tuned by simple variations of the salt concentrations.[32]

Spray pyrolysis was also successfully used in a one-pot synthesis of double-shelled rattles. Using solely tin oxalate as a precursor, water as a solvent, and sucrose as a source of carbon, all of which were heated at 1000 °C for 22 s, resulted in polycrystalline SnO_2@SnO_2@SnO_2 without the need for any post-synthesis treatment. The formation of yolk–shell structures was highly dependent on the presence of sucrose, without which only solid SnO_2 spheres could be obtained. In the proposed mechanism, voids were formed as a result of unequal supply of oxygen to different parts of the initially formed C–SnO_2 composite and thus its unequal combustion to SnO_2. In addition, the temperature dictated the speed of this combustion and as a result determined whether only one or two shells were formed.[24] Using this method, binary (TiO_2–Al_2O_3), ternary (TiO_2–Al_2O_3–ZrO_2), quaternary (TiO_2–Al_2O_3–ZrO_2–CeO_2), and also quinary (TiO_2–Al_2O_3–ZrO_2–CeO_2–Y_2O_3) systems with yolk–shell structures could be obtained.[25]

3.1.3.2. Two-step spontaneous assembly of hydrolytically formed subunits: An innovative approach for a one-pot synthesis of V_2O_5 was developed by Pang et al.[92] As shown in Figure 6, a precursor of vanadium oxide was initially mixed

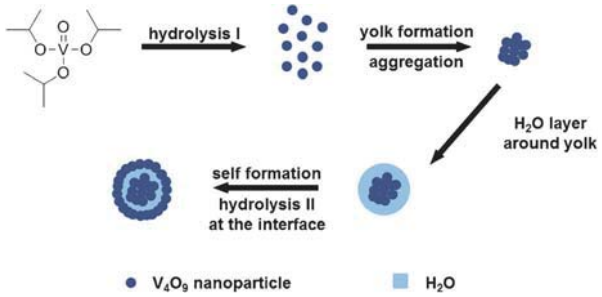

Figure 6. Preparation of nanorattles by two-step spontaneous assembly of hydrolytically formed subunits. On the basis of ref. [92].

with isopropanol in order to decelerate its subsequent hydrolysis in the presence of minor amounts of water. During solvothermal treatment at 190 °C, small V_4O_9 NPs were fabricated, which showed a tendency to aggregate. Those aggregates formed yolks, which are probably surrounded by isopropanol. The weak polarity of the alcohol gave rise to water solvation and secondary hydrolysis probably occurred at the boundary between aqueous and alcoholic phases, leading to the yolk–shell structures. Crystalline V_2O_5 was obtained as a result of subsequent calcination at 500 °C for 30 min.[92]

3.2. Encapsulation sequence

Depending on whether the core or the shell is fabricated first, nanorattle production can be classified by either a bottom-up or top-down approach, regardless of the template used. In the bottom-up approach, a shell is grown around the already pre-

pared core, and therefore can be considered as direct encapsulation. In the top-down approach, the procedure is reversed with the shell being produced first.[39,51]

3.2.1. Bottom-up encapsulation

The bottom-up procedure, also named pre-core-post-shell,[93] for the preparation of core@shell nanocomposites is the most frequently used method nowadays.[14,21,26,31,44,45] In general, the core is first produced[94] by one of many available methods for the preparation of solid nanoparticles.[6b,95] Then, the formed core is encapsulated by the shell. As already described, encapsulation can be carried out by several different methods (Figures 2, 3a and c) by using the microemulsion (section 1.3.1.2) or hard template methods (1.3.1.1). As cores frequently serve as nucleation centers for the subsequent growth of the shell around them, this method is relatively facile compared with the top-down-encapsulation approach, where certain precautions are required to ensure the initial entrance of the core precursors into the formed nanocontainer and their retention before the subsequent formation of the core, as will be described in the next section.

3.2.2. Top-down encapsulation

In the top-down procedure, also called the pre-shell-post-core method,[93] the shell of the nanorattle is prepared first. Afterwards, metal cations are reduced to their metallic form in the void. In this approach, metal precursors can be either encapsulated during[9] or after[18,29] formation of the shell (Figure 3b). As before, let us consider Au@SiO_2 nanorattles prepared by the microemulsion (soft template)[9] and hard template methods.[29]

As shown in Figure 7a, hollow silica spheres with an amino-functionalized inner shell surface (made by the hard template approach) were immersed in an aqueous solution containing $[AuCl_4]^-$ ions. Those ions can diffuse into the void through pores and form chelates with the amino groups. Under hydrothermal treatment, Au^{3+} is reduced to Au^0 in the form of approximately 30 nm AuNPs encapsulated inside the nanocontainer (diameter = 360 nm, wall thickness = 40 nm) with fine Au nanocrystals embedded in the shell as well.[29]

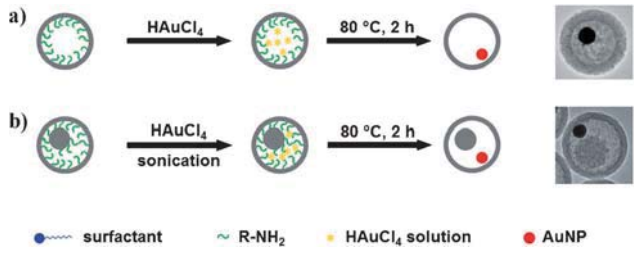

Figure 7. Top-down approach for incorporation of AuNPs into already prepared a) hollow[29] and b) yolk–shell spheres[18] with amine-functionalized interiors to form Au@SiO_2.

Reverse micelles are formed when the aqueous phase is in the minority; thus, water is located inside the micelles.[7] However, substituting water with an aqueous solution of chloroauric acid ($HAuCl_{4(aq)}$) allows introduction of a gold precursor into the system even before the shell precursors (TEOS and APTMS) are added (Figure 3b). These gold precursors remain inside the micelle during the formation of the silica shell and subsequent purification as they are absorbed inside the silica shell.

The reduction to metallic gold occurs upon addition of an aqueous solution of $NaBH_4$. Notably, the amount of encapsulated AuNPs depends on the initial $HAuCl_4$ concentration. At lower concentrations, only one AuNP per shell was produced, whereas at higher concentrations, several AuNPs were encapsulated. After calcination at 560 °C for 6 h, single-Au@SiO_2 did not appear to change, whereas in the case of multiple-Au@SiO_2, the cores sintered, forming larger single-Au@SiO_2. This method thus enables the formation of hollow silica spheres with a diameter of 21.8 ± 2.1 nm filled with AuNPs of tunable size (2.8–4.5 nm) as well as loading (1.2–4.9 wt %).[9]

As seen from the aforementioned examples, when only gold is encapsulated inside a silica shell, the microemulsion method allows preparation of much smaller nanorattles, the total size of which can be smaller than that of just the gold core made by the hard template method. However, the use of the hard template method does not exclude the possibility of obtaining finer AuNPs. For example, SiO_2@SiO_2 nanorattles were prepared by selective etching of the middle layer between the core and the shell, a layer that was composed of TSD—a molecule containing plenty of residual alkylamino groups (Figure 7b). Those groups have the tendency to reduce gold cations under heating[18] as was shown in the previous example.[29] The so-obtained nanorattles were composed of two cores: 50 nm SiO_2 and size-tunable AuNPs (6.9 ± 1.3, 15.1 ± 2.2, 25.4 ± 3.9 nm) surrounded by a 110 nm SiO_2 shell with a 13 nm thick wall.[18]

Further comparing both methods, the success of encapsulation by the microemulsion method relies on the solubility of $HAuCl_4$ in water, which comprises the interior of the reverse micelle.[9] In the case of nanocontainers being prepared by the hard template method, the diffusion of the gold precursor through the pores into the interior plays a crucial role.[18,29] Worth noticing is the fact that, in all cases, the size of AuNPs was simply tuned by variations of the $HAuCl_4$ concentration.[9,18,29]

In the aforementioned examples, all nanorattles consist of an Au core and a SiO_2 shell, and factors such as the choice of the method and silica precursors as well as internal composition of the nanorattle determined the size of the core, shell, and wall thickness. As the optical properties of AuNPs are strictly related to their sizes,[18,29] it should be kept in mind that changes in the experimental procedure can have a large influence on the resulting products and thus possible applications.

Changing the precursor concentration is not the only possibility to control the core size. Hah et al. showed that by repeating the procedure for incorporation of cations into the shell and their subsequent reduction, it is possible to tune the core size. In this way, Cu@SiO_2 nanorattles with cores of 40, 70, and 100 nm were obtained.[51]

Another interesting example of the top-down approach towards encapsulation is associated with the multistep prepara-

tion of thermoresponsive, luminescent nanorattles for controlled drug release (section 6.1.).[57] First, hollow mesoporous silica shells were prepared by the sacrificial hard template method and air was evacuated from the void under vacuum. Then, gadolinium and europium precursors were sucked into the interior. Subsequent calcination at 550 °C led to the formation of gadolinium oxide doped with europium cations. To obtain thermoresponsive P(NIPAm-co-AAm) polymers, the monomers as well as a photoinitiator were encapsulated with the aid of vacuum in a similar way. Exposing the purified nanorattles to UV-light resulted in a photoinduced polymerization inside the void and thus polymer located in between the core and the shell. Fluorescent nanorattles were obtained by silanization with fluorescent silica precursor, whereas drug loading was achieved by soaking for 24 h.[57]

3.2.3. Changing the core

In the previous sections, methods of core incorporation were presented. An alternative approach to core formation is metal displacement, a method that provides an interesting way to exchange already encapsulated metal cores for another metal. For example, $Cu@SiO_2$ can be transformed into $Ag@SiO_2$ by a redox reaction in which zero-valent CuNPs are oxidized to Cu^{2+} cations while Ag^{+} cations are reduced to metallic Ag inside the core.[51]

3.3. Void formation

3.3.1. Selective removal

In the previous subchapters, we have already seen diversified approaches to building nanorattle structures. Most of those methods, however, do not provide direct formation of yolk–shell structures and core–shell nanoparticles are formed instead. The common procedures to reach yolk–shell structures involve a) removal of the interlayer;[10,15,19,21,26,27,31,34,37,46,48,53,60,67] b) partial removal of the shell;[70] c) partial[12,29,30,96] or complete[29,57,83] removal of the core; d) removal of unreacted chemicals from the void.[9,14] Depending on the nature of the compartment intended to be removed, in general, either a chemical[10,29,30,45] or a thermal[31,34,54] treatment is applied.

Chemical removal usually involves the use of aqueous solutions[15,21,27,30,45,46,48,55,56,60,67] as well as organic solvents.[71,72] In the case of silica nanorattles, differences in density between the silica building blocks are widely used. Porous compartments are less dense and thus more susceptible to etching than denser ones. The different porosities are generally obtained due to differences in structure or composition. In the first case, the presence of surfactants and co-surfactants leads to the formation of silica shells with different porosity even when a single silica precursor (TEOS) is used.[26] In the second case, the combination of silanes with organosilanes plays a crucial role.[10] For example, hybrid silica spheres composed of an inorganic core and an outer layer with a middle layer containing organosilica frameworks was transformed into yolk–shell structures upon etching with HF.[10] For the removal of silica compartments, hot water,[56,67] solutions of HF,[10,19,53,70] Na_2CO_3,[26,29] NH_4OH,[27,30,45] NaOH,[15,21,46,48,55,60] $KMnO_4$,[66] and/or organosilane-assisted etching[23,69] are normally used. For example, Yang et al. demonstrated a one-pot transformation of $Fe_3O_4@SiO_2$ and $Au@SiO_2$ core–shell nanoparticles into yolk–shell ones by using an organosilane-assisted selective etching method. As the Si–O–Si bonds of silica shells obtained from TEOS in $metal@SiO_2$ core–shell nanoparticles were disordered owing to the short reaction time, the balance between hydrolysis and condensation was disturbed upon addition of organosilane precursors. The outer layer of the silica shell was probably protected from hydrolysis by deposited organosilica, whereas the silica network closer to the core was broken and gradually replaced by moieties of organosilanes.[69] The opposite mechanism was proposed by Zhang et al.,[29] wherein SiO_2 cores prepared by hydrolysis and condensation of TEOS by the Stöber method[88] are the factors determining the size as well as the polydispersity of further obtained nanorattles. These cores can be subsequently functionalized with amino groups by hydrolysis and co-condensation of APTES and TEOS. During mild etching with Na_2CO_3, the solid silica core is dissolved. The resistance of the shell towards etching is provided by the presence of carbon chains (originating from organosilane) located on the inner and outer surface of the shell. These chains can contain, for example, nitrogen and hydrogen atoms able to form hydrogen bonds with each other. The so-formed hydrophobic layer protects the silica framework from the aqueous etching.[29] The void can also be formed by self-etching of silica. For instance, treatment of an $Au@SiO_2$ core–shell nanoparticle with mild aqueous ammonia leads to partial dissolution of the shell and formation of silicate anions. Those anions react further with metal cations, resulting in the formation of Au@metal silicate yolk–shell structures.[44] In the case of nanorattles prepared by microemulsions, a void was obtained either by soaking in water for a few days[14] or by washing with hot water for 40 min.[9,33] Moreover, PVP can be used in the so-called "surface-protected etching" process. In this process, the silica compartment is removed either by hot water treatment[67,97] or by concentrated NaOH at room temperature.[98]

Removal of metal (Ni[12]) and metal oxide (Fe_3O_4[57]) cores is usually done by etching with HCl. Dissolution of a Fe_3O_4 core by $NaBH_4$ catalyzed by AuNPs has been reported as well.[83] A silver interlayer can be dissolved by oxidation with H_2O_2.[37] Despite the toxicity of KCN, it can be efficiently used for partial or complete removal of Au cores.[96,99]

When polystyrene beads are used as a hard template, they can be removed by dissolution with organic solvents such as toluene[71] or xylene.[72] In the case of thermal removal of organic compartments, a poly(methyl acrylic acid (PMAA) inter layer is decomposed to form the void, whereas the organic component of $C_{18}TMS$ forms pores during pyrolysis (500 °C, 6 h).[31] The polymeric carbon can be calcinated at 400 °C in 2 h.[34]

3.3.2. Chemical transformation

3.3.2.1. Galvanic displacement: Galvanic displacement, also called galvanic replacement, is a method based on the fact

that different metals exhibit different electrical potentials.[38] As a result of redox reactions, metal@metal (Au@Pt,[49] Au@Au[36,100]), metal@alloy (Au@$Au_{0.52}Ag_{0.48}$, Au@$Pd_{0.65}Ag_{0.35}$, Au@$Pt_{0.43}Ag_{0.57}$)[101] and alloy@alloy (Au/Ag@Au/Ag[102]) nanorattles can be obtained. As shown in Figure 8, a core–shell sphere

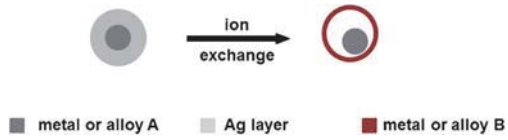

Figure 8. Preparation of nanorattles by galvanic replacement.

composed of a metal[36,49] or alloy[102] core coated with a layer of metallic Ag constitutes the basis for the preparation of nanorattles. Subsequent chemical treatment leads to the replacement of the metallic shell by another metal[36,49,100] or an alloy.[102] This is a facile method to obtain nanorattles with super-thin shells. The size of the void between core and shell can be easily tuned by the initial thickness of the Ag layer.[102] Therefore, this layer plays a dual role; as a sacrificial template as well as a reducing agent.

Preparation of metal@metal nanorattles is done, for example, by displacing metallic silver in Au@Ag core–shell spheres with Pt by using H_2PtCl_6, leading to their conversion into yolk–shell Au@Pt nanorattles.[49] For alloy@alloy preparation, Au/Ag@Au/Ag nanorattles with a diameter of approximately 70 nm were prepared by treating Au/Ag@Ag core–shell nanoparticles with $HAuCl_4$ solution at 100 °C.[102] Dealloying of silver follows the redox reaction:[36]

$$3\,Ag^0 + [AuCl_4]^- \rightarrow Au^0 + 3\,Ag^+ + 4\,Cl^- \quad (2)$$

To avoid possible precipitation of AgCl on the surface of the fabricated nanorattles,[36,38] the reaction needs to be carried out at elevated temperatures and diluted concentrations of reagents. In comparison, the use of copper as a sacrificial template excludes the formation of insoluble byproducts and allows the synthesis tom occur at room temperature, as in the case of Pd@Au_xCu_{1-x}.[38]

3.3.2.2. Kirkendall effect: The Kirkendall effect is a phenomenon in which an interface between two species moves upon heating due to the different diffusion rates of ions or atoms in these two species.[103] The occurrence of hollow structures through the Kirkendall effect originates from the generation and migration of vacancies, that is, empty lattice sites. Owing to the different diffusion rates of atoms/ions, these lattice vacancies form voids and their growth leads to the formation of hollow structures.[104] For example, metal oxide hollow spheres can be fabricated from metal nanoparticles during oxidation: an initially formed thin layer of metal oxide on the nanoparticle surface constitutes an interface between metal and oxygen. As oxidation proceeds, those two species can diffuse through the interface. This includes out-diffusion of metal ions or atoms and in-diffusion of oxygen. If the out-diffusion proceeds significantly faster than the in-diffusion, the inner part of the nanoparticle becomes empty, leading to hollow spheres.[105] Accordingly, in the case of core–shell nanoparticles, the transformation of the shell results in yolk–shell nanoparticles (Figure 9). An early report by Yin[106] showed, for example, the formation of yolk–shell Pt@CoO by mixing Pt nanocrystals with

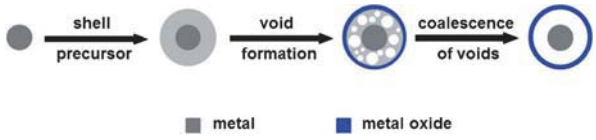

Figure 9. Preparation of nanorattles through the Kirkendall effect.

a $Co_2(CO)_8$ solution and the subsequent oxidation at elevated temperature.[106] Crystalline Ag@γ-Fe_2O_3 nanorattles have been obtained by oxidation as well. This was done by mixing AgNPs, as a seed source, and $Fe(CO)_5$ as an iron precursor, with a 1-octadecane solution containing oleylamine under inert conditions. Heating of the mixture to 250 °C in the presence of air for 2 h resulted in the formation of nanorattles.[52]

Recently, Qin et al. demonstrated a two-step ion-exchange method to form cubic CdS nanorattles. In the first step, anion exchange transforms solid AgCl nanocubes into Ag_2S. The speed of S^{2-} ion addition is crucial and determines the further structure. Upon fast injection of sulfide solutions, yolk–shell nanoboxes are obtained, whereas dropwise addition results in the formation of hollow nanoboxes. This indicates that both anion diffusion as well as the Kirkendall effect contribute to the formation of a hollow void. In the second step, silver cations are exchanged by cadmium cations. In a similar way, PbS, ZnS, and $AgInS_2$ nanoboxes can be obtained.[41]

4. Importance of Nanorattle Building Blocks in the Design of Future Applications

The possible applications of nanorattles are inherently associated with their structure as well as their composition. As mentioned in section 2, metal particles such as Au, Pt, Pd are often used as catalysts. On the other hand, nanorattles with iron oxide cores are often used for targeted drug delivery because of their magnetic properties. The cores are protected from agglomeration and aggregation,[21,31,32,40,44,45] sintering,[15,60] and interaction with the surrounding environment.[9,30] An additional feature provided by the shell is the presence of pores, which enable the transport of molecules inside and outside the nanocontainer across the shell.[23,57] The void, on one hand, provides a homogenous environment[21] for reactions and, on the other hand, a storage capacity for encapsulated cargo.[57,107] And, last but not least, depending on the chemical composition, the core,[23] shell[23,26,27,31,52] as well as void[30] can be functionalized.

4.1. Core

Converse to core–shell nanoparticles, the cores of nanorattles are not located in the center of the nanocontainer: often they tend to stick to the inner layer of the shell when observed

under the vacuum conditions of TEM. Therefore, they are believed to be freely movable.[26,31,35,45,55,59,70,98,108] In an experiment by Sun et al., Au/Ag@Au/Ag nanorattles were deposited on TEM grids at two different tilting angles, 0° and 70°. As the ratio of the cores located at the bottom and at the top of the shells varied depending on the tilting angle, movement of the cores upon solvent evaporation was suggested.[102]

Purity is crucial for efficient action of a catalytically active core. Thus, templates and surfactants used in the preparation of nanorattles should be completely removed. Otherwise, the catalytic sites of the core can be capped, which later hinders its catalytic activity.[40] This was seen, for example, in the case of multi-yolk PdNPs encapsulated in mesoporous CeO_2, which were tested towards catalytic CO oxidation. Nanorattles calcinated at 550 °C exhibited slightly better performance than the ones calcinated at 350 °C.[21]

4.2. Shell

4.2.1. Protecting role

Although numerous reports praise the beneficial role of the shell, only rarely has this been proven experimentally. Several studies have reported the significance of the shell in preventing sintering of the encapsulated core, for example, in the cases of Au@TiO_2,[48,60] Au@ZrO_2,[15,60] Au/TiO_2@ZrO_2,[60] Au@SiO_2,[9] and Pd@CeO_2.[21] The importance of the shell to preserve the core's catalytic properties was investigated by Arnal et al., where Au@ZrO_2 nanorattles were crushed under high pressure (1 GPa) and subsequently calcinated at 800 °C. TEM images of these samples revealed that the AuNPs sintered, leading to particle size enlargement. Furthermore, crushed Au@ZrO_2 used in the oxidation of CO resulted in significantly poorer catalytic performance than non-crushed calcinated Au@ZrO_2. This is due to the fact that in the latter case, AuNPs were well preserved in the shell and had not sintered during the thermal treatment, which clearly indicates a protecting role of the ZrO_2 shell upon thermal treatment.[15]

As mentioned already in section 3.2.2., if several AuNPs are encapsulated in one silica shell, they tend to sinter and form one bigger AuNP at elevated temperatures. Notably, this sintering is entirely limited to within the shell confinement and does not occur between neighboring nanocontainers.[9,32]

The protecting role of the silica shell against catalytic poisoning was tested by treating Au@SiO_2 nanorattles with *meso*-2,3-dimercaptosuccinic acid (DMSA) and then determining their catalytic properties in the reduction of 4-nitrophenol. As a control experiment, citrate-capped AuNPs were tested in the same way. After poisoning, almost all catalytic activity of Au@citrate vanished owing to the ligand exchange of citrate by DMSA. In contrast, Au@SiO_2 nanorattles merely showed a slight decrease in activity upon DMSA treatment as only some DMSA could diffuse into the interior of the nanocontainer. This is due to the fact that the high pH resulting from the excess of reducing agent leads to repulsive interaction between negatively charged DMSA (deprotonated) and Au@SiO_2 (zeta potential = −43.2 mV), thus hindering diffusion of DMSA into the void.[9]

4.2.2. Mediator with external environment

Pores located on the shell act as channels connecting the void of the sphere with the external environment. Thanks to their presence, transport into and out of nanocontainers is possible.[23,40,57] Lee et al. demonstrated that the shell acts as the determining factor in nanorattle-driven kinetics. For instance, in the catalytic conversion of CO in the presence of Au@TiO_2, an induction time of 10 min was observed before oxidation occurred. This retardation may be attributed to diffusion limits between the shell exterior and interior.[48] Moreover, Liang et al. showed recently that small molecules such as CO and larger ones like cinchonidine are able to easily diffuse in and out of yolk–shell and core–shell nanospheres made of titania and silica. Therefore, when considering possible future applications of nanocomposites, one should bear in mind this aspect. In the case of catalysis, rapid diffusion is desirable. In the case of drug delivery, however, certain precautions should be taken to prevent unwanted drug release.[46] Similarly, there are cases where blockage of pores is desirable. This, for example, can be used to prevent direct contact between the silicon core and the electrolyte in the case of lithium-ion batteries.[19]

4.2.3. Encapsulation of cargo

The encapsulation of drugs,[26,27,31,54,57,68,109] core precursors,[18,29,51,55,57,93] and functional interlayers[57] in the interior of already prepared nanorattles or hollow spheres is usually done by one of two approaches. Both approaches are based on the diffusion of dissolved molecules into the void through pores in the shell. In the first case, dried nanorattles are soaked in a solution containing the intended cargo. This loading method usually includes incubation,[27] agitation,[31,109] sonication with stirring,[26,29,51] sonication alone,[18] or stirring alone.[54,55,57,68,110] In the second approach, encapsulation can additionally be facilitated by removal of any air or solution residing in the cavity of the nanocapsule after its preparation and purification process. This is done by applying vacuum and subsequent incorporation of the cargo.[57] Moreover, to ensure retention of water-insoluble drugs inside the rattle, the void can be functionalized to exhibit hydrophobic properties.[27]

4.3. Void

It is known that the void provides a homogenous environment.[40] In addition, some reports demonstrate that its size can be controlled.[19,34,111] However, no significant focus has been devoted to the role of the void so far.[30] Recently, however, it was shown that the size of the void can effect some properties, such as the speed of catalytic reactions driven by Fe_2O_3@mSiO_2 (m = mesoporous).[34] Cui et al. demonstrated that the larger the void, the faster the degradation of methylene blue (MB). This was reflected by the fact that increasing the void space from 5 nm to 16 and 40 nm resulted in increased dye degradation from 62% to 70% and 90%, respectively. The increased catalytic properties were attributed to the fact that more MB can accumulate inside the void.[34]

A sufficiently large and rigid void is important in cases where the core changes its volume, as occurs when alloy anodes of Li-ion batteries undergo a lithium insertion/extraction process.[19, 32, 111]

Hydrophobic voids can be prepared by silylation of compartments with silica precursors containing long carbon chains, for example, C_{18}TES[30] and C_{18}TMS.[27] Additionally, using a precursor with branched organic chains, such as IBMS, superhydrophobic shells can be obtained.[70]

5. Nanorattle Characterization

As mentioned, the building blocks of the nanorattles determine their properties and thus influence their potential applications. Therefore, it is crucial to know the exact chemical composition as well as the structure of the prepared nanorattles. It is well known that the characterization of nanomaterials should always include more than one technique owing to the limitations of the used methods. Thus, special care should be taken in the choice of adequate methods as well as the interpretation of the results.

5.1. Composition of the nanorattles

There are several methods to determine the composition of nanorattles. The method best suited depends on the nature of the nanorattle properties, such as crystallinity, magnetism, or luminescence. The presence of noble metals, such as Ag[33] and Au,[9, 18, 29, 31, 37, 83] can be verified by simple UV/Vis spectroscopy due to their surface plasmon resonance. The content of the metallic core (Ag,[33] Au,[9, 18] Fe,[52, 54] Pd[61]) in the nanorattle or the composition of alloy nanorattles[101] can be determined by, for example, inductively coupled plasma optical-emission spectroscopy (ICP-OES).

The composition of crystalline nanorattles is normally determined by X-ray diffraction (XRD),[8, 9, 12, 19, 21, 23, 26–29, 31, 32, 40, 41, 44, 45, 51, 53, 56, 57, 69, 83, 87, 92] or X-ray powder diffraction (XRPD),[61] energy-dispersive X-ray spectroscopy (EDS or EDX), or wide-angle XRD.[18] Sometimes, however, strong background signals from the amorphous silica shell can hinder the detection of the encapsulated core at low core contents, as shown in a study by Zhu et al., where the XRD pattern of the crystalline Fe_3O_4 core could only be observed after dissolution of the silica shell.[54] Furthermore, we have observed that XRPD does not detect small amounts of metallic silver present in Ag@SiO_2 nanorattles. Therefore, the presence of AgNPs can be only detected by UV/Vis spectroscopy. Alternatively, increased loading with AgNPs results in clearly visible Ag peaks in the diffractograms.[33]

In the case of rattles containing organic residues, their content can be verified by thermal analysis, such as thermogravimetric analysis and differential thermal analysis, TGA-DTA.[10, 27, 31, 55, 87, 89]

Fourier transform infrared spectroscopy (FTIR) is frequently used for the detection of functional groups.[23, 26, 29–31, 40, 45, 55, 57, 87] However, if some components, such as molecules attached into the surface, are only present in small amounts, their presence might not be detected.[55] Furthermore, encapsulation can lead to a significant weakening of the bands corresponding to the cargo as well.[87] With regard to composites containing $-NH_2$ groups, their content can be quantified by the Kaiser assay,[10] or a fluorenylmethyloxycarbonyl (FMOC) quantification protocol.[26] Less frequently used but powerful methods include UV-Raman spectroscopy,[23] ^{13}C cross-polarization magic-angle spinning (CP-MAS) nuclear magnetic resonance (NMR) spectroscopy[23] and ^{29}Si CP-MAS NMR spectroscopy.[69]

In the case of magnetic-compartment-containing rattles, such as those with Fe_3O_4[8, 30, 55, 69, 87, 109] and Fe_2O_3,[27, 31] a magnetization hysteresis loop is frequently measured. It should be noticed that the saturation magnetization is decreased when nonmagnetic layers are built around magnetic iron oxide.[8, 55, 87]

The presence of fluorescent dyes[26] and folic acid[27] can usually be detected by UV/Vis spectroscopy,[26, 27] whereas FITC[26] and luminescent particles like Gd_2O_3[57] are measured by photoluminescence spectroscopy.

As already mentioned, the charge of the particle surface changes depending of the presence of functional groups[10] and coatings.[68] This influences the zeta potential (ζ-potential) as well as the stability of nanorattles. For measurement of the ζ-potential, dynamic light scattering (DLS)[68, 110] is usually used.

5.2. Proof of core encapsulation

Transmission electron microscopy (TEM) is the most frequently used method for determining whether the obtained nanoparticles are nanorattles or not.[8–10, 12, 14, 15, 18–26, 28–32, 34, 35, 37, 40–42, 44, 45, 48, 49, 51–57, 60, 61, 66, 69, 70, 83, 87, 89, 91, 92, 101, 109, 112, 113] As electrons traverse the specimen, it is possible to distinguish between regions of varying electron density. In general, compartments with higher electron density appear darker compared with those of lower electron density.[114] For example, Ag@SiO_2 nanorattles appear to be composed of a darker core and a brighter shell.[33] In the case of a silica core coated with layers of silica functionalized with organic groups,[10] no difference could be observed in the TEM, but removal of the middle layer led to the formation of a bright void.[10] In situ TEM is a powerful technique to study the progress of reactions.[19] In the work of Liu et al., for instance, it was successfully used to show the electrochemical lithiation of Si@C nanorattles and for observing the size expansion of the core.[19]

Scanning electron microscopy (SEM) is often used for the visualization of the morphology[8, 10, 19, 22, 24–26, 28, 29, 34, 40–42, 44, 45, 56, 66, 69, 83, 87, 89, 91, 92, 109, 112, 113] of the sample and in many cases, images of broken spheres with the core located inside provide proof of encapsulation.[10, 24, 92, 113] Usually, the core of the rattle is invisible when using SEM.[8, 28, 29, 32, 44, 45, 66, 83, 113] However, working at elevated acceleration voltages (5 kV,[26] 10 kV[10]) may enable visualization of the core.[10, 22, 26, 32] Converse to TEM, the more electron dense elements appear brighter than less electron dense elements, which appear dark. For example, gold in Au@SiO_2 nanorattles is far brighter than its surrounding silica shell.[29] Sometimes other electron microscopes such as high-angle annular dark-field scanning TEM (HAADF-STEM) can be used.[8, 18, 38, 52, 57]

SEM and TEM are often coupled to EDS,[23,28,29,38,41,44,45,54–57] enabling elemental mapping of nanorattles. This technique can be particularly useful when other detection methods fail in the assessment of chemical composition.

X-ray photoelectron spectroscopy (XPS) allows the characterization of surface composition[18,19,26,28,40,52] with a detection depth limit of approximately 10 nm.[18,28] Therefore, if the shell thickness exceeds this value, any encapsulated cargo will not be detected; thus, this can prove encapsulation. In this case, however, another method should also be used to confirm the presence and nature of the encapsulated core. For example, in a study by Zhang et al., TEM of Pt@CeO_2 demonstrated a rattle structure, EDS confirmed the presence of Pt, Ce, and O, whereas XPS showed only Ce and O, thus additionally confirming the encapsulation of Pt.[28] However, in a study by Tan et al., the silica nanorattles were of much smaller size and had thinner shells than the aforementioned rattles so the presence of the Au core could be detected by XPS.[18] In conclusion, there should always be a combination of different methods for the characterization of nanorattles.

5.3. Surface area and porosity

Nitrogen absorption–desorption isotherms allow the determination of the specific surface area (SSA) of nanorattles,[8–10,21,23,26,27,29–31,40,45,53,54,56,57,61,66,69,87,109,112] whereas the pore distribution can be addressed by the Barett–Joyner–Haleda (BJH) method.[10,21,26,27,29–31,54,66,69,112] These parameters are especially crucial when considering potential applications. The specific surface area is generally related to the size of the pore volume. Thus, it largely depends on the presence of molecules attached to or absorbed on the surface. For example, magnetic iron oxide encapsulated in mesoporous silica has a specific surface area of 494.5 $m^2 g^{-1}$, which decreases significantly to 120.3 $m^2 g^{-1}$ after attachment of PEG and folic acid (FA) conjugates. However, the presence of a large hysteresis loop between absorption and desorption shows the presence of an accessible cavity structure, which is necessary for further drug loading.[31] Similarly, Kang et al. showed that a gradual decrease in pore volume, surface area, and pore diameter was the result of step-wise loading of hollow mesoporous silica spheres with a Gd_2O_3:Eu^{3+} core, a thermoresponsive polymer, and subsequently with a drug.[57]

5.4. Loading with cargo

Loading of nanocontainers with a drug as well as its release can be determined by UV/Vis spectroscopy in case of UV/Vis-active drugs.[26,31,37] For example, loading can be measured indirectly by calculating the difference between the concentration of the drug in the initial solution and in the remaining supernatant after loading.[31] Another method to verify loading with a drug is FTIR,[54,57] which indicates the presence of the functional groups of the drug, whereas thermogravimetric analysis (TGA) allows determination of the weight content of the drug.[54] However, when using UV/Vis spectroscopy and TGA for determination of drug loading, one should take into consideration the possible presence of molecules attached to the nanocontainer surface rather than encapsulated within, the presence of which can be due to not only drug but also impurities or surfactants as well. In addition, single differential thermal analysis (SDTA) could serve as an elegant complementary method to determine the temperature differences of samples under heating.[115] Cargo absorbed on the surface should, in general, decompose earlier than the encapsulated cargo.

6. Applications

Already several reviews have focused on the properties and possible applications of nanorattles.[16,116] Thus, we will focus on some more recent examples of these applications as well as highlight the superior performance of nanorattles compared with traditional nanoparticles. Owing to the diversity of the possible combinations of the building blocks, research is increasingly focused on applications in areas of social and economic interest, such as drug delivery, catalysis, and Li-ion batteries. Although magnetic solid-phase extraction, high-performance microwave absorbers, and antimicrobial nanorattles currently constitute a niche area based on the amount of publications, they may well find broader application in the future.

6.1. Drug delivery

Development of new materials to efficiently fight cancer still remains an eminent challenge, and high requirements are imposed on nanoparticles intended to serve as drug carriers. Nanoparticles that act solely as storage and transport for drugs is not sufficient in terms of efficient treatment; therefore, novel nanodrugs often exhibit several additional functionalities. Rattles with magnetic cores[27] and ligands for cellular receptors[27,31] located on the shell surface are intended for targeted drug delivery. Visualization of the nanocontainers can be achieved either by magnetic resonance imaging (MRI)[27] or functionalization with fluorescent dyes.[26] In addition, the latest generation of smart nanorattles is equipped with stimuli-responsive mechanisms.[57] As will be shown, only nanorattles composed of silica shells are of the interest for biomedical applications so far.

After encapsulation of maghemite γ-Fe_2O_3 into mesoporous silica (γ-Fe_2O_3@SiO_2), the surface of the shell can be further grafted with PEG, which is a biocompatible polymer, and with FA, widely used for tumor targeting. These nanorattles can be efficiently loaded with an anti-cancer drug, such as doxorubicin hydrochloride (DOX), with a relatively large loading capacity of 220 $\mu g\, mg^{-1}$ and slowly release the drug over 67 h.[31] As DOX is released rapidly only during first 6 h and subsequently its release is significantly slower, this rattle-type carrier could possibly be used in small doses to avoid flooding patients' bodies with a drug and at the same time provide a constant cancer treatment.

Nanorattles of 200 nm SiO_2@SiO_2 were fluorescently labelled and pegylated, then tested for applications in drug delivery as well as cell imaging. After penetrating the plasma membrane, these nanorattles were found in the cytoplasm of cancer cells

(cell line MDA-MB-231) with some located inside lysosomes. As determined by an MTT assay using 3-(4,5-dimethylthiazol-2-yl)-2,5-diphenyltetrazolium bromide, no significant cytotoxicity was observed after 1 and 2 days when concentrations of up to 200 $\mu g\,mL^{-1}$ were applied, showing their promising biocompatibility. As determined by UV/Vis spectroscopy, 44.25 μg of DOX can be loaded into 1 mg of functionalized nanorattles, with a loading efficiency of 70.8%. The speed of drug release was strictly pH dependent as it was observed that after 107 h at pH 4.8, 45% of drug was released, whereas at pH 7.4 only 17% was released. This was attributed to the protonation and deprotonation of the amine groups of the drug, leading to altered electrostatic interactions with the mesoporous silica. DOX-loaded nanorattles showed extraordinary cytotoxicity, even at concentrations as low as 3.125 $\mu g\,mL^{-1}$, the toxicity of which was time dependent and increased with longer incubation times.[26]

Although DOX is a frequently studied drug for encapsulation in nanorattles,[26,31] it is not the only one being tested. For example, ferromagnetic Fe_3O_4@mSiO_2 (m = mesoporous) can be efficiently loaded with aspirin (27.7 wt%).[54] The aspirin-loaded rattles were characterized by initial fast drug release within the first 12 h, which gradually decelerated with time. As with the aforementioned fluorescent SiO_2@SiO_2 nanorattles loaded with DOX, the release was highly pH dependent. In contrast to DOX, aspirin release was higher at high pH, which was related to its higher solubility at high pH.[54]

Another example of nanorattles with a magnetic Fe_3O_4 core was reported by Wu and co-workers.[27] A hydrophobic void was obtained by use of a silica precursor containing *n*-octadecyl groups, whereas conjugation with PEG and FA provided surface functionality. The cytotoxicity and cellular uptake towards two cancer cell lines, namely HeLa and MCF-7, were studied. These magnetic mesoporous silica nanorattles showed low toxicity and folate-receptor-mediated uptake. Loading with docetaxel (DOC) resulted in significant cytotoxicity towards both cell lines with the HeLa cells showing higher cytotoxicity. This was probably due to enhanced uptake owing to the overexpression of folate receptors on the HeLa cell surface, a process that does not occur in the case of MCF-7 cells. Superior cytotoxicity of encapsulated DOC over the free drug showed the evident and advantageous role of the shell. As the interior of the nanorattle is hydrophobic, the water-insoluble drug can be efficiently loaded inside the nanocontainers. Once they are taken up, the drug is released in the hydrophobic parts of the cellular compartments. In vivo tests showed that these magnetic nanocontainers can be guided to the tumor location by use of an external magnet, a process that resulted in increased uptake (0.24 mg of Fe per gram liver weight) compared to the uptake in the absence of an external magnetic field (0.18 mg of Fe per gram liver weight). All functionalities provided by the core (magnetic), void (hydrophobic), and shell (containing ligands), make these nanorattles an attractive means of targeting drug delivery as well as for magnetic resonance imaging.[27]

The aforementioned nanorattles might serve as potential vectors in drug delivery primarily because of the possibility of loading drugs in their cavities. These drugs can then be released over quite long periods of time.[26,31,54] In many cases, however, controlled drug release is more desirable. As several materials have been reported to respond to external stimuli, such as temperature, pH, ionic strength, magnetic field, ultrasound, and enzymes, they have potential for such medical applications.[117,118] A lot of focus has been devoted to polymers because of their temperature-responsive ability to reversibly undergo a phase transition.[118,119] For example, PNIPAm (poly(*N*-isopropylacrylamide)) is swollen below 32 °C, whereas above this temperature, the polymer shrinks.[120] This feature can be effectively utilized in the temperature-responsive opening of shell pores. Kang et al. produced hybrid nanorattles composed of an inorganic Gd_2O_3:Eu^{3+} core and a silica shell with an organic polymer layer in between.[57] These hybrids did not show significant toxicity towards SKOV3 ovarian cancer cells. Additionally, fluorescently labelled nanorattles were shown to be taken up and localized in the cytoplasm. Owing to the presence of Gd, those composites might serve as potential contrast agents in MRI. Then, a non-steroidal, anti-inflammatory drug, indomethacin (IMC), was loaded into the rattles with and without PNIPAm polymer. In absence of the hydrogel, the drug was constantly released regardless of the applied temperature (20 °C and 45 °C). In the presence of the polymer layer, however, IMC release was observed only at higher temperature (45 °C), whereas at lower temperature (20 °C), the release was completely blocked. This temperature-responsive behavior is probably due to water absorption as well as volume expansion at 20 °C, which led to the filling of the channels and the void, thus preventing the drug from being released. When the temperature is increased, the polymer shrinks, channels are opened, and IMC is squeezed out from the hydrogel network. Interestingly, Gd_2O_3:Eu^{3+} photoluminescence was highly dependent on the concentration of the loaded drug. Therefore, these nanorattles can also function as tracing or detecting agents.[57]

Silica nanorattles also demonstrate potential as vaccine adjuvants.[110] In a study by Liu et al., a model protein, ovalbumin (OVA), was loaded on SiO_2 nanorattles, mesoporous SiO_2 NPs, and solid SiO_2 NPs for comparison. Greater amounts of protein were absorbed on the nanorattles compared with the other silica particles. The positive charge on the surface of the nanorattles, as well as the presence of the void, contributed to a relatively high loading content of 14.76%. Treating murine macrophage cell lines with these nanorattles at concentrations in the range 6.25–400 $\mu g\,mL^{-1}$ did not affect cell viability. Likewise, regardless of the concentration of the nanorattles used (10, 25 and 50 $mg\,kg^{-1}$), the immune organs of mice, that is, the spleen and thymus, did not demonstrate any abnormalities 14 days after the last injection. OVA-loaded nanorattles stimulated the immune response of mice, leading to increased levels of OVA-specific IgG antibodies. Interestingly, those levels were considerably higher (OD = 0.42) than those resulting from treatment solely with OVA (OD = 0.11). Good in vitro and in vivo biocompatibility of these nanorattles, as well as the elevation of the OVA antibody level after single dose vaccination, make those nanorattles promising candidates for vaccine adjuvants.[110]

In this section, it was shown that nanorattles intended for drug delivery are of increasing interest. Despite promising results, more studies still need to be performed in vitro and in vivo to exclude long-term adverse effects. Additionally, owing to the strict Food and Drug Administration regulations, it might take decades before nanorattles become standard agents in medical treatment. On the other hand, the rising number of lifestyle diseases will certainly drive science in the direction of more and more "intelligent" materials—a group that multifunctional nanorattles certainly belong to.

6.2. Confined nanoreactors

The unique properties offered by nanorattles (protecting shell and void) are evidently of great importance for confined nanoreactors. In the following section, it will be shown that nanorattles can be effectively used in catalysis and cascade reactions. Furthermore, we will demonstrate that these smart materials predominantly exhibit a great advantage over solid NPs or core–shell NPs in terms of performance.

6.2.1. Heterogeneous catalysis

Nanoparticles, such as Au,[9,15,18,31,44,48,60] Ni,[12] Pd,[21,53,61] and Ag,[33] are known to demonstrate catalytic properties. However, aggregation, occurring under harsh conditions, constitutes a major problem in terms of their application.[21,31] This problem can be overcome by encapsulation of these NPs inside hollow spheres. The shell provides a physical barrier between the encapsulated cargo and the exterior as well as providing a relatively homogenous environment in the cavity.[9,21]

Several nanorattles containing AuNPs have been reported.[9,15,18,31,60] Their catalytic properties were tested for the reduction of, for example, 2-nitroaniline[18] and 4-nitrophenol.[9,70] It was demonstrated that the silica shell provides a sufficient means for the prevention of aggregation.

Wu et al. investigated the dependency of the size of the AuNPs on the catalytic properties. To do so, three Au@SiO_2 nanorattles with increasing core size (2.8 ± 0.7, 3.3 ± 0.6, and 4.5 ± 0.7 nm) were tested in the reduction of 4-nitrophenolate. It was shown that the rate constants were inversely proportional to the size of the nanoparticles (3.1×10^6, 2.4×10^6, and 9.5×10^5 $min^{-1} mole^{-1}$, respectively), thus clearly indicating that the smaller the AuNPs, the higher their catalytic activity.[9]

As shown in the above-mentioned example, the catalytic properties of AuNPs are highly size dependent.[9] Nevertheless, Park et al. showed that in hydrogen-transfer reactions, there is only a slight difference in reactivity between Ni@SiO_2 nanorattles with core sizes of 3 and 30 nm.[12]

In cases where the AuNPs are the same size, the hydrophobicity of the shell plays a crucial role in the catalysis of reactions of organic compounds in an aqueous phase. First, in the catalytic reduction of 4-nitrophenol, it was shown that the reaction was faster in the case of AuNPs encapsulated in superhydrophobic isobutyl-functionalized silica (Au@IB-YSN) than those encapsulated in mesoporous silica and carbon. Then, comparing the reaction rates of Au@IB-YSN in the catalytic reduction of 2-methyl-4-nitrophenol and 2,6-dimethyl-4-nitrophenol, it was demonstrated that the higher the hydrophobicity of the substituted nitrophenol, the higher the reaction rate.[70]

Silica is not the only agent that can be used to prevent aggregation of catalytically active nanoparticles: Au@ZrO_2[15,60] as well as Au@TiO_2[48,60] have been reported as catalysts for CO oxidation. Although the latter surpasses the former in catalytic performance, the doping of Au@ZrO_2 with small quantities of TiO_2 (0.6, 3.1, and 5.6 wt%) leads to a significant improvement of their properties with the rule that the larger the doping, the lower the temperature of half CO conversion, meaning a higher activity.[60]

Chen et al. reported novel nanorattles composed of hollow mesoporous CeO_2 spherical compartments with multiple voids that contain individual Pd nanoparticles (Pd@hm-CeO_2). These nanocomposites, calcinated at 350 °C and 550 °C, were tested in catalytic CO oxidation reactions. Both sets of nanorattles showed 100% conversion of carbon monoxide at only 110 °C, with the rattles calcinated at the higher temperature exhibiting a slightly better performance at lower reaction temperatures. This might be due to an improved surface cleaning of PdNPs upon the calcination at higher temperatures. Despite the fact that hm-CeO_2 alone does not promote this CO oxidation at all, its synergetic effect with PdNPs becomes evident when the Pd@hm-CeO_2 activity is compared with that of PdNPs supported on SiO_2. Therefore, the significance of the ceria shell is reflected in its dual role as an agent preventing aggregation and sintering of PdNPs at high temperatures—increasing their stability and recyclability—and as an agent with a reactive surface that enhances the catalytic properties of the core.[21]

A Fenton-like reaction is a reaction where Fe^{3+} and H_2O_2 are used in combination. During this reaction, oxidative radicals are generated, such as hydroxyl radicals (•OH). As they oxidize organic compounds to water and carbon dioxide, Fenton-like reagents can be used in wastewater treatment.[121] Cui et al., for instance, investigated Fe_2O_3@mSiO_2 nanorattles in the oxidation of methylene blue (MB). Empty silica shells demonstrated an ability to reduce the dye concentration by 30% within the first hour, whereas bare spindle α-Fe_2O_3 caused only a 20% concentration decrease after 7 h. This clearly shows the poor performance of the latter as a potential Fenton-like reagent. In the case of the empty nanocontainers, the drop in MB concentration was probably due to adsorption of the dye during the initial stage of the incubation, as the concentration remained nearly constant afterwards. Conversely, nanorattles showed a high activity (up to 90%) with oxidation of the dye progressing over 7 h. Indeed, this activity was eminently dependent on the size of the void, with the tendency that the larger the void space, the more efficient the degradation of MB.[34]

Another example is provided by Kim et al., who emphasized the importance of shell porosity in Suzuki coupling reactions catalyzed by encapsulated PdNPs. Pd@SiO_2 core–shell, two Pd@SiO_2-NiPhy, and Pd@NiPhy yolk–shell nanoparticles with increasing pore volume and surface area were tested in the reaction of 1-bromo-4-ethylbenzene with phenylboronic acid to 4-

ethylbiphenyl. Pd@NiPhy showed the highest conversion efficiency and Pd@SiO_2 the lowest. This was apparently related to pore volumes and thus diffusion rates through them. As mentioned before, the shell plays a protecting role for the core to avoid agglomeration. In designing future applications of nanorattles, a long life span of the shell should be taken into consideration, and it should survive harsh reaction conditions. This was shown, for instance, in a recycling test of Pd@NiPhy and Pd@SiO_2. Although the former still gave complete conversion after five cycles, the catalytic performance of the latter decreased significantly. This was due to partial dissolution of the silica shell and agglomeration of PdNPs under the basic conditions of the reaction mixture.[53]

As a concluding remark for this section, it was shown that nanorattles act as an attractive alternative to traditional catalysts that suffer from loss of activity due to agglomeration and sintering under harsh reaction condition. The role of the shell is limited mainly to protection of the encapsulated core and allows pore size control; only in rare cases can enhance catalytic properties.

6.2.2. Photocatalysis

In the search for more economically friendly reactions, photocatalysis is gaining interest.[122] By using Pt@CeO_2, benzyl aldehyde can be obtained under mild conditions (room temperature, ambient pressure) by the selective oxidation of benzyl alcohol. The process is driven by visible light and the presence of PtNPs significantly enhances the poor photocatalytic properties of the CeO_2 shell. It is worth pointing out that the core–shell type of nanocomposites exhibit much higher activity than nanorattles in this case. This can be explained by differences in interfacial charge transfer: as the interfacial distance between the core and shell in core–shell Pt@CeO_2 is spatially dense, it leads to longer charge carrier lifetimes compared with yolk–shell Pt@CeO_2, where the contact between components is quite loose.[28]

Photocatalytic degradation of methylene blue can be carried out by SiO_2@$NiTiO_3$ nanorattles. After only 2.5 h, 90% of the dye is degraded. This makes nanorattles much more efficient photocatalysts than $NiTiO_3$ nanoparticles, in which case the degradation reached solely 22%. The superior photocatalytic activity of nanorattles compared with $NiTiO_3$ hollow spheres implies that the silica core is significant.[45] This observation is in agreement with a previous study by Li et al., where it was demonstrated that microrattles showed significantly higher photocatalytic activity than hollow and solid spheres in the degradation of phenol. Interestingly, yolk–shell spheres showed difference in catalytic performance depending on the size of the core. These unique properties originate from multiple reflections of light within the interior cavity[113] and clearly show that the design determines the further properties.

Photocatalysts such as TiO_2 can be used for the purification of water from organic materials through their degradation. The environmental concern remains, however, due to the potential of placing aqueous ecosystems in jeopardy through the presence of TiO_2. Therefore, after treatment the catalyst should be removed. This is possible by fabricating nanorattles composed of magnetic cores with photocatalytic shells, such as Fe_3O_4@TiO_2. Although this catalyst demonstrated lower catalytic activity compared with pure TiO_2 nanoparticles, Degussa P25, their indubitable advantage is the ability to rapidly remove them from solution owing to the presence of the magnetic core. In addition, recyclability measurement showed that although the catalytic performance was decreased after several trials, the nanorattles could be regenerated easily by exposing them to UV light.[56]

6.2.3. Electrocatalysis

Au@Pt can be used as an electrocatalyst for the oxidation of methanol to CO_2 under basic conditions. Electrochemical properties were compared with other catalysts. The nanorattles showed the highest specific activity compared with Au@Pt core–shell, hollow Pt, PtNPs, as well as commercial Pt/C. In addition, yolk–shell Au@Pt demonstrated high CO tolerance, which might be attributed to the presence of a gold core and the void.[49]

6.2.4. Cascade reactions

As seen in the examples of nanorattles used in catalysis, the potential of the shell is not fully exploited and, in most cases, the main attention is usually given solely to the properties of the core. Recently, Yang et al. reported nanorattles with a precise functionalization of both compartments in such a way that the core exhibited basic properties due to the presence of $-NH_2$ groups, while the shell contained acidic groups (SO_3H). These nanomaterials were tested in a deacetalization/Henry cascade reaction and their performance was compared with nanorattles with a) only an acidic silica shell (SiO_2@SO_3H), b) only a basic core (NH_2@ethanesilica) and c) a mixture of SiO_2@SO_3H and NH_2@ethanesilica.

Figure 10 shows the deacetalization, which is catalyzed by SO_3H groups (step 1), and the Henry reaction, which is cata-

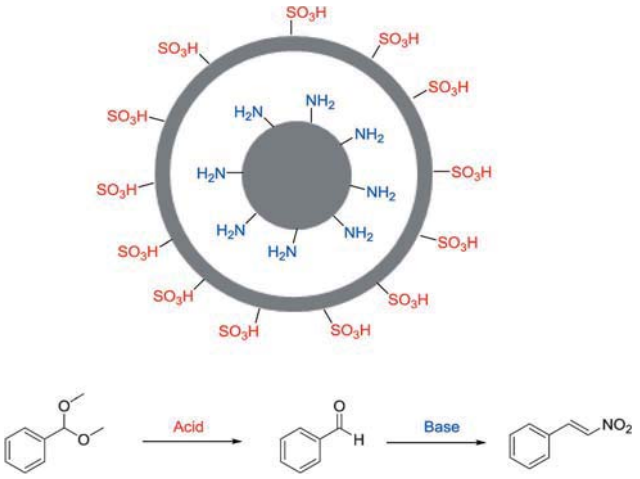

Figure 10. Deacetalization/Henry cascade reaction catalyzed by NH_2@SO_3H nanorattles.

lyzed by NH_2 groups (step 2). As a result of its structural properties, SiO_2@SO_3H could catalyze only step 1 of this cascade reaction, whereas in the case of NH_2@ethanesilica, no reaction occurred owing to the absence of benzyl aldehyde. Both NH_2@SO_3H as well as the mixture of SiO_2@SO_3H and NH_2@ethanesilica yielded nitrostyrene, showing that both steps occurred. The higher yield of nitrostyrene, in the case of the reaction catalyzed by NH_2@SO_3H (>99%) in comparison to the mixture (55%), was attributed to different reaction routes. In the former case, a short distance between the catalytic moieties within this nanoreactor played a crucial role. In addition, this distance seemed to be ideal as the sulfonic moieties of shells and the amine moieties of the cores do not neutralize each other. In the case of the mixture, however, the reaction pathway lengthens as formed benzylaldehyde needs to diffuse from SiO_2@SO_3H to NH_2@ethanesilica. With regard to recyclability, NH_2@SO_3H demonstrated high catalytic activity even after the 2nd and 3rd cycles, with 88% and 72% yields of nitrostyrene, respectively.[23]

6.3. Li-batteries

Along with the increasing demand for rechargeable batteries, improvement of lithium and lithium-ion batteries is gaining more and more interest.[123] Anodes used in lithium-ion batteries can be typically either graphite-type or alloy-type (such as Si and Sn), with the former dominating the market even though the latter demonstrate higher Li-storage capacity. This is due to the formation of a solid-electrode interphase (SEI) film, which forms on the surface of anodes while the organic electrolyte is reductively decomposed. The formed film breaks on the surface of the alloy electrodes as the anode volume expands and contracts while Li is inserted or extracted. As a result, cracks are exposed at the interface of the electrode with the electrolyte, leading to further growth and formation of a thick SEI layer during the cycling procedure. This process is clearly unfavorable due to the constant consumption of the electrolyte and thus, drying of the cell.[19]

Si@carbon nanorattles can provide an attractive possibility to overcome the problem of SEI rupture in the aforementioned electrodes. In this system, the encapsulated Si core is physically separated from the SEI film located on the outer layer of the carbon shell. At the same time, the void provides space for the alloy to change in volume without destroying the SEI film. As determined by in situ TEM, the Si core expands upon electrochemical lithiation. Its enlargement, however, does not cause rupture of the carbon shell.[19]

Sn@carbon might also serve as a promising candidate for anode materials in lithium batteries.[32,111] When comparing nanorattles differing significantly in the size of the encapsulated particles, the diameter of the rattle, as well as the size distribution,[32,111] the differences in electrochemical performance show that the method used is of great importance in terms of further applications.

The preparation of more complex nanocomposites, such as SnO_2@carbon hollow spheres with embedded Sn nanoparticles, increases the reversible capacity. These ameliorated cycling abilities and exceptional capacities, compared with Sn@carbon alone, can be attributed to, among others, SnO_2 nanoplates enhancing the charge transfer and decreasing the transport distance for electrons and lithium cations. Thanks to these properties, the aforementioned hybrid appears to be an excellent candidate for application in lithium-ion batteries.[111]

Additionally, electrodes produced with double-shelled SnO_2@SnO_2@SnO_2 nanorattles showed better electrochemical properties compared with the ones prepared with solid SnO_2. This extraordinary capacity to store lithium is due to the high porosity of the material as well as the presence of the void. Nevertheless, the above-mentioned SEI film was formed on the surface of both SnO_2 electrodes.[24]

6.4. Magnetic solid-phase extraction

Magnetic solid-phase extraction is a relatively new method for the separation and preconcentration of components from large volumes of solutions.[124] Recently, Zeng et al. reported a rattle-type microsphere with a magnetic-carbon double-layered shell that demonstrated potential to detect trace organic targets in environmental water. In this system, the hydrophobic interior of the nanorattle was obtained by functionalization of the SiO_2 core and the inner Fe_3O_4 layer with C_{18} groups. The outer carbon layer plays a dual role: on one hand, it protects the Fe_3O_4 layer from the surrounding environment; on the other hand, it provides a surface with numerous adsorption sites for extraction of trace analytes. The performance of the so-composed sorbents was determined by the extraction of toxic polycyclic aromatic hydrocarbons (PACs). Interestingly, it was observed that if the sorbent is used in high amounts, there is almost no difference in extraction efficacy between nanorattles functionalized with C_{18} groups and non-functionalized ones. Conversely, functionalized nanorattles showed superior extraction capacity at low concentrations of the nanorattle. This clearly indicates that the C_{18} groups significantly enhance the properties of the aforementioned adsorption sites on the outer carbon layer.[30]

6.5. High performance microwave absorbers

Recently, Liu et al. showed for the first time the potential of double-shelled rattles as high performance microwave absorbers. These materials are composed of a magnetic core (Fe_3O_4) surrounded by a dielectric double shell (SnO_2). The double-shelled rattles, naked solid Fe_3O_4, core–shell Fe_3O_4@SiO_2, as well as single-shell Fe_3O_4@SiO_2 rattles were tested for their ability to absorb microwaves. Greater microwave absorption was observed with increasing complexity of the tested material for the bare core, core–shell, and single-shell rattles. Interestingly, when the core was surrounded by a double layer, the absorption could be enhanced even more depending on the spheres' parameters such as size, void, and wall thickness. The above-mentioned microwave absorption was attributed to, among others, a synergistic role of core and shell as well as the presence of the void.[8]

6.6. Antimicrobial nanorattles

Wei et al. prepared Ag@γ-Fe_2O_3 nanorattles conjugated with glucose through a dopamine anchor. Owing to the presence of this monosaccharide, the nanorattles could specifically target *Escherichia coli* ER2566. The magnetic shell allowed the physical removal of attached bacteria from the medium. In addition, owing to the presence of AgNPs, these nanorattles showed antimicrobial properties against *Escherichia coli* O157:H7 and *Bacillus subtilis*.[52]

In our group, we have prepared Ag@SiO_2 nanorattles that exhibit good antimicrobial properties against *Escherichia coli* K 12 TH14515. As the silica shell is functionalized with the NH_2 groups, these nanorattles can be functionalized with fluorescent dyes or attached to a surface.[125]

7. Conclusion

Rapid progress of nanotechnology within the last several decades has favored the creation of nanostructures with increasing levels of complexity. As was shown in this Review, various methods that are frequently used for the preparation of solid nanoparticles also constitute a basis for the development of micro- and nanorattles as well. Although solid nanoparticles have received relatively a lot of work, nanorattles still remain a niche area to be further explored. Their undoubtable advantages over traditional NPs result mainly from the presence of the void, which allows movement of the encapsulated core as well as its protection, factors that subsequently contribute to the enhanced properties of nanorattles.

The current literature gives a growing number of impressive examples, but these results are not always directly comparable owing to different materials, different measurement conditions, different aspects/influences, and/or frequently incomplete sample characterization. Therefore, it is of great importance to establish precise guidelines for standard testing of these new materials to facilitate research by scientists all over the world.

We anticipate an increasing trend in research focused on the preparation of multifunctional nanorattles. As frequently emphasized, particle size governs their properties. Bearing in mind the potential offered by nanorattles in industrial and medical applications, research with significant focus on simple, eco-friendly, scalable methods leading to the formation of monodisperse samples is expected.

Acknowledgements

We would like to thank the University of Fribourg, the Fribourg Center for Nanomaterials FriMat and the Swiss National Research Foundation for the generous funding of the project. This project was carried within The National Research Programme NRP-62 “Smart Materials”.

Keywords: nanofabrication · nanoparticles · nanorattles · smart nanomaterials · yolk–shell nanoparticles

[1] a) R. P. Feynman, *Eng. Sci.* **1960**, 22 – 36; b) K. E. Drexler, *Bull. Sci. Technol. Soc.* **2004**, *24*, 21 – 27.
[2] C. Toumey, *Nat. Nanotechnol.* **2009**, *4*, 783 – 784.
[3] I. Freestone, N. Meeks, M. Sax, C. Higgitt, *Gold Bull* **2007**, *40*, 270 – 277.
[4] a) M.-C. Daniel, D. Astruc, *Chem. Rev.* **2004**, *104*, 293 – 346; b) S. Eckhardt, P. S. Brunetto, J. Gagnon, M. Priebe, B. Giese, K. M. Fromm, *Chem. Rev.* **2013**, *113*, 4708 – 4754; c) N. L. Rosi, C. A. Mirkin, *Chem. Rev.* **2005**, *105*, 1547 – 1562; d) C. Burda, X. Chen, R. Narayanan, M. A. El-Sayed, *Chem. Rev.* **2005**, *105*, 1025 – 1102.
[5] a) K. Ariga, T. Mori, S. Ishihara, K. Kawakami, J. P. Hill, *Chem. Mater.* **2014**, *26*, 519 – 532; b) S. E. Skrabalak, J. Chen, Y. Sun, X. Lu, L. Au, C. M. Cobley, Y. Xia, *Acc. Chem. Res.* **2008**, *41*, 1587 – 1595; c) K. Sun, T.-S. Wei, B. Y. Ahn, J. Y. Seo, S. J. Dillon, J. A. Lewis, *Adv. Mater.* **2013**, *25*, 4539 – 4543; d) M. Imboden, H. Han, J. Chang, F. Pardo, C. A. Bolle, E. Lowell, D. J. Bishop, *Nano Lett.* **2013**, *13*, 3379 – 3384; e) C. Joachim, G. Rapenne, *ACS Nano* **2013**, *7*, 11 – 14.
[6] a) G. Schmid, *Nanoparticles: From theory to application*, Wiley-VCH, Weinheim, **2010**; b) C. Altavilla, E. Ciliberto, *Inorganic nanoparticles: Synthesis applications, and perspectives*, CRC Press, Boca Raton, **2011**; c) D. L. Feldheim, C. A. Foss, *Metal nanoparticles: Synthesis characterization, and applications*, Marcel Dekker, New York, **2002**.
[7] D. Ganguli, M. Ganguli, *Inorganic particle synthesis via macro- and microemulsions: A micrometer to nanometer landscape*, Kluwer Acad./ Plenum Publishing, New York, **2003**.
[8] J. Liu, J. Cheng, R. Che, J. Xu, M. Liu, Z. Liu, *J. Phys. Chem. C* **2013**, *117*, 489 – 495.
[9] S.-H. Wu, C.-T. Tseng, Y.-S. Lin, C.-H. Lin, Y. Hung, C.-Y. Mou, *J. Mater. Chem.* **2010**, *20*, 789 – 794.
[10] D. Chen, L. Li, F. Tang, S. Qi, *Adv. Mater.* **2009**, *21*, 3804 – 3807.
[11] Y. Yin, C. Erdonmez, S. Aloni, A. P. Alivisatos, *J. Am. Chem. Soc.* **2006**, *128*, 12671 – 12673.
[12] J. C. Park, H. J. Lee, J. Y. Kim, K. H. Park, H. Song, *J. Phys. Chem. C* **2010**, *114*, 6381 – 6388.
[13] a) S.-H. Hu, X. Gao, *J. Am. Chem. Soc.* **2010**, *132*, 7234 – 7237; b) A. Walther, A. H. E. Müller, *Soft Matter* **2008**, *4*, 663; c) A. Walther, A. H. E. Müller, *Chem. Rev.* **2013**, *113*, 5194 – 5261.
[14] Y.-S. Lin, S.-H. Wu, C.-T. Tseng, Y. Hung, C. Chang, C.-Y. Mou, *Chem. Commun.* **2009**, 3542 – 3544.
[15] P. M. Arnal, M. Comotti, F. Schüth, *Angew. Chem. Int. Ed.* **2006**, *45*, 8224 – 8227; *Angew. Chem.* **2006**, *118*, 8404 – 8407.
[16] M. Pérez-Lorenzo, B. Vaz, V. Salgueiriño, M. A. Correa-Duarte, *Chem. Eur. J.* **2013**, *19*, 12196 – 12211.
[17] Z. Chen, Z.-M. Cui, P. Li, C.-Y. Cao, Y.-L. Hong, Z.-y. Wu, W.-G. Song, *J. Phys. Chem. C* **2012**, *116*, 14986 – 14991.
[18] L. Tan, D. Chen, H. Liu, F. Tang, *Adv. Mater.* **2010**, *22*, 4885 – 4889.
[19] N. Liu, H. Wu, M. T. McDowell, Y. Yao, C. Wang, Y. Cui, *Nano Lett.* **2012**, *12*, 3315 – 3321.
[20] K. A. Dahlberg, J. W. Schwank, *Chem. Mater.* **2012**, *24*, 2635 – 2644.
[21] C. Chen, X. Fang, B. Wu, L. Huang, N. Zheng, *ChemCatChem* **2012**, *4*, 1578 – 1586.
[22] X.-J. Wu, D. Xu, *Adv. Mater.* **2010**, *22*, 1516 – 1520.
[23] Y. Yang, X. Liu, X. Li, J. Zhao, S. Bai, J. Liu, Q. Yang, *Angew. Chem. Int. Ed.* **2012**, *51*, 9164 – 9168; *Angew. Chem.* **2012**, *124*, 9298 – 9302.
[24] Y. J. Hong, M. Y. Son, Y. C. Kang, *Adv. Mater.* **2013**, *25*, 2279 – 2283.
[25] Y. J. Hong, M. Y. Son, B. K. Park, Y. C. Kang, *Small* **2013**, *9*, 2224 – 2227.
[26] G. Song, C. Li, J. Hu, R. Zou, K. Xu, L. Han, Q. Wang, J. Yang, Z. Chen, Z. Qin, *J. Mater. Chem.* **2012**, *22*, 17011 – 17018.
[27] H. Wu, G. Liu, S. Zhang, J. Shi, L. Zhang, Y. Chen, F. Chen, H. Chen, *J. Mater. Chem.* **2011**, *21*, 3037 – 3045.
[28] N. Zhang, X. Fu, Y.-J. Xu, *J. Mater. Chem.* **2011**, *21*, 8152 – 8158.
[29] K. Zhang, H. Chen, Y. Zheng, Y. Chen, M. Ma, X. Wang, L. Wang, D. Zeng, J. Shi, *J. Mater. Chem.* **2012**, *22*, 12553 – 12561.
[30] T. Zeng, X. Zhang, Y. Ma, S. Wang, H. Niu, Y. Cai, *Chem. Commun.* **2013**, *49*, 6039 – 6041.
[31] B. Liu, J. Wang, S. Sun, X. Wang, M. Zhao, W. Zhang, H. Zhang, X. Yang, *RSC Adv.* **2013**, *3*, 18506 – 18518.
[32] R. Zheng, X. Meng, F. Tang, L. Zhang, J. Ren, *J. Phys. Chem. C* **2009**, *113*, 13065 – 13069.
[33] M. Priebe, K. M. Fromm, *Part. Part. Syst. Charact.* **2013**, *31*, 645 – 651.
[34] Z.-M. Cui, Z. Chen, C.-Y. Cao, L. Jiang, W.-G. Song, *Chem. Commun.* **2013**, *49*, 2332 – 2334.

[35] X.-J. Wu, D. Xu, *J. Am. Chem. Soc.* **2009**, *131*, 2774 – 2775.
[36] Y. Khalavka, J. Becker, C. Sönnichsen, *J. Am. Chem. Soc.* **2009**, *131*, 1871 – 1875.
[37] E. Choi, M. Kwak, B. Jang, Y. Piao, *Nanoscale* **2013**, *5*, 151 – 154.
[38] S. Xie, M. Jin, J. Tao, Y. Wang, Z. Xie, Y. Zhu, Y. Xia, *Chem. Eur. J.* **2012**, *18*, 14974 – 14980.
[39] Z. Wang, D. Luan, C. M. Li, F. Su, S. Madhavi, F. Y. C. Boey, X. W. Lou, *J. Am. Chem. Soc.* **2010**, *132*, 16271 – 16277.
[40] N. Yan, Q. Chen, F. Wang, Y. Wang, H. Zhong, L. Hu, *J. Mater. Chem. A* **2013**, *1*, 637 – 643.
[41] Z. Qin, H. Sun, Z. Jiang, X. Jiao, D. Chen, *CrystEngComm* **2013**, *15*, 897 – 902.
[42] H. B. Wu, A. Pan, H. H. Hng, X. W. D. Lou, *Adv. Funct. Mater.* **2013**, *23*, 5669 – 5674.
[43] W. Cho, Y. H. Lee, H. J. Lee, M. Oh, *Adv. Mater.* **2011**, *23*, 1720 – 1723.
[44] K. Dong, Z. Liu, J. Ren, *CrystEngComm* **2013**, *15*, 6329 – 6334.
[45] W. Dong, Y. Zhu, H. Huang, L. Jiang, H. Zhu, C. Li, B. Chen, Z. Shi, G. Wang, *J. Mater. Chem. A* **2013**, *1*, 10030 – 10036.
[46] X. Liang, J. Li, J. B. Joo, A. Gutiérrez, A. Tillekaratne, I. Lee, Y. Yin, F. Zaera, *Angew. Chem. Int. Ed.* **2012**, *51*, 8034 – 8036; *Angew. Chem.* **2012**, *124*, 8158 – 8160.
[47] Y. Hu, X. T. Zheng, J. S. Chen, M. Zhou, C. M. Li, X. W. Lou, *J. Mater. Chem.* **2011**, *21*, 8052 – 8056.
[48] I. Lee, J. B. Joo, Y. Yin, F. Zaera, *Angew. Chem. Int. Ed.* **2011**, *50*, 10208 – 10211; *Angew. Chem.* **2011**, *123*, 10390 – 10393.
[49] L. Kuai, S. Wang, B. Geng, *Chem. Commun.* **2011**, *47*, 6093 – 6095.
[50] S. N. Shmakov, E. Pinkhassik, *Chem. Commun.* **2010**, *46*, 7346 – 7348.
[51] H. J. Hah, J. I. Um, S. H. Han, S. M. Koo, *Chem. Commun.* **2004**, 1012 – 1013.
[52] Z. Wei, Z. Zhou, M. Yang, C. Lin, Z. Zhao, D. Huang, Z. Chen, J. Gao, *J. Mater. Chem.* **2011**, *21*, 16344 – 16348.
[53] M. Kim, J. C. Park, A. Kim, K. H. Park, H. Song, *Langmuir* **2012**, *28*, 6441 – 6447.
[54] Y. Zhu, E. Kockrick, T. Ikoma, N. Hanagata, S. Kaskel, *Chem. Mater.* **2009**, *21*, 2547 – 2553.
[55] B. Shi, J. Ren, X. Liu, G. Lu, Y. Wang, *Synt. Met.* **2012**, *162*, 1443 – 1450.
[56] S. Linley, T. Leshuk, F. X. Gu, *ACS Appl. Mater. Interfaces* **2013**, *5*, 2540 – 2548.
[57] X. Kang, Z. Cheng, D. Yang, P. Ma, M. Shang, C. Peng, Y. Dai, J. Lin, *Adv. Funct. Mater.* **2012**, *22*, 1470 – 1481.
[58] M. Kim, K. Sohn, H. B. Na, T. Hyeon, *Nano Lett.* **2002**, *2*, 1383 – 1387.
[59] G. L. Li, C. A. Tai, K. G. Neoh, E. T. Kang, X. Yang, *Polym. Chem.* **2011**, *2*, 1368 – 1374.
[60] R. Güttel, M. Paul, F. Schüth, *Catal. Sci. Technol.* **2011**, *1*, 65 – 68.
[61] J. C. Park, E. Heo, A. Kim, M. Kim, K. H. Park, H. Song, *J. Phys. Chem. C* **2011**, *115*, 15772 – 15777.
[62] a) R. Ciriminna, A. Fidalgo, V. Pandarus, F. Béland, L. M. Ilharco, M. Pagliaro, *Chem. Rev.* **2013**, *113*, 6592 – 6620; b) Y. Chen, H.-R. Chen, J. L. Shi, *Acc. Chem. Res.* **2014**, *47*, 125 – 137.
[63] A. van Blaaderen, A. Vrij, *J. Colloid Interface Sci.* **1993**, *156*, 1 – 18.
[64] J. Vicente, M.-T. Chicote, R. Guerrero, P. G. Jones, M. C. Ramírez de Arellano, *Inorg. Chem.* **1997**, *36*, 4438 – 4443.
[65] K. E. Sapsford, W. R. Algar, L. Berti, K. B. Gemmill, B. J. Casey, E. Oh, M. H. Stewart, I. L. Medintz, *Chem. Rev.* **2013**, *113*, 1904 – 2074.
[66] Q. Yu, J. Hui, P. Wang, X. Wang, *Inorg. Chem.* **2012**, *51*, 9539 – 9543.
[67] W. Fan, B. Shen, W. Bu, F. Chen, K. Zhao, S. Zhang, L. Zhou, W. Peng, Q. Xiao, H. Xing, *J. Am. Chem. Soc.* **2013**, *135*, 6494 – 6503.
[68] L. Li, Y. Zhang, N. Hao, D. Chen, F. Tang, *Chin. Sci. Bull.* **2012**, *57*, 3631 – 3638.
[69] Y. Yang, J. Liu, X. Li, X. Liu, Q. Yang, *Chem. Mater.* **2011**, *23*, 3676 – 3684.
[70] S. Shi, M. Wang, C. Chen, J. Gao, H. Ma, J. Ma, J. Xu, *Chem. Commun.* **2013**, *49*, 9591 – 9593.
[71] A. Imhof, *Langmuir* **2001**, *17*, 3579 – 3585.
[72] A.-H. Pei, Z.-W. Shen, G.-S. Yang, *Mater. Lett.* **2007**, *61*, 2757 – 2760.
[73] H. Gröger, F. Gyger, P. Leidinger, C. Zurmühl, C. Feldmann, *Adv. Mater.* **2009**, *21*, 1586 – 1590.
[74] H. Gröger, C. Kind, P. Leidinger, M. Roming, C. Feldmann, *Materials* **2010**, *3*, 4355 – 4386.
[75] C. Zimmermann, C. Feldmann, M. Wanner, D. Gerthsen, *Small* **2007**, *3*, 1347 – 1349.
[76] D. H. M. Buchold, C. Feldmann, *Nano Lett.* **2007**, *7*, 3489 – 3492.
[77] C. Zurmühl, R. Popescu, D. Gerthsen, C. Feldmann, *Solid State Sci.* **2011**, *13*, 1505 – 1509.
[78] P. Leidinger, R. Popescu, D. Gerthsen, H. Lünsdorf, C. Feldmann, *Nanoscale* **2011**, *3*, 2544 – 2551.
[79] P. Leidinger, R. Popescu, D. Gerthsen, C. Feldmann, *Small* **2010**, *6*, 1886 – 1891.
[80] C. Kind, R. Popescu, E. Müller, D. Gerthsen, C. Feldmann, *Nanoscale* **2010**, *2*, 2223 – 2229.
[81] F. Gyger, M. Hübner, C. Feldmann, N. Barsan, U. Weimar, *Chem. Mater.* **2010**, *22*, 4821 – 4827.
[82] P. Leidinger, N. Dingenouts, R. Popescu, D. Gerthsen, C. Feldmann, *J. Mater. Chem.* **2012**, *22*, 14551 – 14558.
[83] K. M. Yeo, J. Shin, I. S. Lee, *Chem. Commun.* **2010**, *46*, 64 – 66.
[84] S.-H. Chung, D.-W. Lee, M.-S. Kim, K.-Y. Lee, *J. Colloid Interface Sci.* **2011**, *355*, 70 – 75.
[85] K. R. Henke, *Arsenic: Environmental chemistry, health threats and waste treatment*, Wiley, Chichester, **2009**.
[86] a) Y. Waseda, S. Suzuki, *Characterization of corrosion products on steel surfaces*, Springer, Heidelberg, **2006**; b) I. T. Lucas, E. Dubois, J. Chevalet, S. Durand-Vidal, S. Joiret, *Phys. Chem. Chem. Phys.* **2008**, *10*, 3274.
[87] F. Lan, H. Hu, W. Jiang, K. Liu, X. Zeng, Y. Wu, Z. Gu, *Nanoscale* **2012**, *4*, 2264 – 2267.
[88] W. Stöber, A. Fink, E. Bohn, *J. Colloid Interface Sci.* **1968**, *26*, 62 – 69.
[89] Y. Xia, L. Xu, *Synt. Met.* **2010**, *160*, 545 – 548.
[90] G. Cao, Y. Wang, *Nanostructures and nanomaterials: Synthesis properties, and applications*, World Scientific, Singapore, **2011**.
[91] L. Cao, D. Chen, R. A. Caruso, *Angew. Chem. Int. Ed.* **2013**, *52*, 9014 – 9018; *Angew. Chem.* **2013**, *125*, 9184 – 9188.
[92] H. Pang, P. Cheng, H. Yang, J. Lu, C. X. Guo, G. Ning, C. M. Li, *Chem. Commun.* **2013**, *49*, 1536 – 1538.
[93] L. Qiang, X. Meng, L. Li, D. Chen, X. Ren, H. Liu, J. Ren, C. Fu, T. Liu, F. Gao, *Chem. Commun.* **2013**, *49*, 7902 – 7904.
[94] a) J. S. Chen, C. Chen, J. Liu, R. Xu, S. Z. Qiao, X. W. Lou, *Chem. Commun.* **2011**, *47*, 2631; b) C. Galeano, R. Güttel, M. Paul, P. Arnal, A.-H. Lu, F. Schüth, *Chem. Eur. J.* **2011**, *17*, 8434 – 8439.
[95] R. Nagarajan, T. A. Hatton, *Nanoparticles: Synthesis stabilization, passivation, and functionalization*, American Chemical Society, Oxford University Press, Washington, DC, **2008**.
[96] J. Lee, J. C. Park, H. Song, *Adv. Mater.* **2008**, *20*, 1523 – 1528.
[97] Y. Hu, Q. Zhang, J. Goebl, T. Zhang, Y. Yin, *Phys. Chem. Chem. Phys.* **2010**, *12*, 11836 – 11842.
[98] Q. Zhang, J. Ge, J. Goebl, Y. Hu, Z. Lu, Y. Yin, *Nano Res.* **2009**, *2*, 583 – 591.
[99] J. Lee, J. C. Park, J. U. Bang, H. Song, *Chem. Mater.* **2008**, *20*, 5839 – 5844.
[100] H. M. Chen, R.-S. Liu, K. Asakura, J.-F. Lee, L.-Y. Jang, S.-F. Hu, *J. Phys. Chem. B* **2006**, *110*, 19162 – 19167.
[101] E. C. Cho, P. H. C. Camargo, Y. Xia, *Adv. Mater.* **2010**, *22*, 744 – 748.
[102] Y. Sun, B. Wiley, Z.-Y. Li, Y. Xia, *J. Am. Chem. Soc.* **2004**, *126*, 9399 – 9406.
[103] L. Cademartiri, G. A. Ozin, *Concepts of nanochemistry*, Wiley-VCH, Weinheim, **2009**.
[104] H. J. Fan, U. Gösele, M. Zacharias, *Small* **2007**, *3*, 1660 – 1671.
[105] G. E. Fryxell, G. Cao, *Environmental applications of nanomaterials: Synthesis sorbents and sensors*, Imperial College Press, London, **2012**.
[106] Y. Yin, *Science* **2004**, *304*, 711 – 714.
[107] L. Li, Y. Guan, H. Liu, N. Hao, T. Liu, X. Meng, C. Fu, Y. Li, Q. Qu, Y. Zhang, *ACS Nano* **2011**, *5*, 7462 – 7470.
[108] a) S. Xing, L. H. Tan, T. Chen, Y. Yang, H. Chen, *Chem. Commun.* **2009**, 1653 – 1654; b) C. C. Yec, H. C. Zeng, *Chem. Mater.* **2012**, *24*, 1917 – 1929.
[109] F. Zhang, G. B. Braun, A. Pallaoro, Y. Zhang, Y. Shi, D. Cui, M. Moskovits, D. Zhao, G. D. Stucky, *Nano Lett.* **2012**, *12*, 61 – 67.
[110] T. Liu, H. Liu, C. Fu, L. Li, D. Chen, Y. Zhang, F. Tang, *J. Colloid Interface Sci.* **2013**, *400*, 168 – 174.
[111] X. Song, J. Pan, L. Xiao, L. Gao, S. Mathur, *Nanotechnology* **2013**, *24*, 205401.
[112] H. Wang, J.-G. Wang, H.-J. Zhou, Y.-P. Liu, P.-C. Sun, T.-H. Chen, *Chem. Commun.* **2011**, *47*, 7680 – 7682.
[113] H. Li, Z. Bian, J. Zhu, D. Zhang, G. Li, Y. Huo, H. Li, Y. Lu, *J. Am. Chem. Soc.* **2007**, *129*, 8406 – 8407.
[114] U. W. Gedde, *Polymer physics*, Chapman & Hall, London, **1995**.

[115] M. E. Brown, *Handbook of thermal analysis and calorimetry*, Elsevier, Amsterdam, **1998**.
[116] a) J. Liu, S. Z. Qiao, J. S. Chen, X. W. Lou, X. Xing, G. Q. Lu, *Chem. Commun.* **2011**, *47*, 12578 – 12591; b) G. Li, Z. Tang, *Nanoscale* **2014**, *6*, 3995 – 4011; c) J. C. Park, H. Song, *Nano. Res.* **2011**, *4*, 33 – 49.
[117] R. Lehner, X. Wang, S. Marsch, P. Hunziker, *Nanomedicine* **2013**, *9*, 742 – 757.
[118] A. S. Hoffman, *Adv. Drug Delivery Rev.* **2013**, *65*, 10 – 16.
[119] F. D. Jochum, P. Theato, *Chem. Soc. Rev.* **2013**, *42*, 7468 – 7483.
[120] R. W. Kelsall, I. W. Hamley, M. Geoghegan, *Nanoscale science and technology*, Wiley, Hoboken, **2005**.
[121] Z. Ai, L. Lu, J. Li, L. Zhang, J. Qiu, M. Wu, *J. Phys. Chem. C* **2007**, *111*, 4087 – 4093.
[122] D. Ravelli, D. Dondi, M. Fagnoni, A. Albini, *Chem. Soc. Rev.* **2009**, *38*, 1999 – 2011.
[123] M. S. Whittingham, *Chem. Rev.* **2004**, *104*, 4271 – 4302.
[124] M. Šafaříková, I. Šafařík, *J. Magn. Magn. Mater.* **1999**, *194*, 108 – 112.
[125] M. Priebe, PhD thesis, University of Fribourg, Switzerland, **2014**.